NASA CR-66427

RESEARCH AND DEVELOPMENT OF MAGNESIUM/ALUMINUM ELECTROFORMING PROCESS FOR SOLAR CONCENTRATORS

By K. Lui, R. Guidotti, and M. Klein

GPO PRICE $ _____

CFSTI PRICE(S) $ _____

Hard copy (HC) _3.00_

Microfiche (MF) _.65_

ff 653 July 65

Prepared under Contract No. NAS1-6218 by

ELECTRO-OPTICAL SYSTEMS, INC.
A Xerox Company
Pasadena, California

for

NATIONAL AERONAUTICS AND SPACE ADMINISTRATION

N67-34490

(ACCESSION NUMBER)   (THRU)

89
(PAGES)

CR-66427
(NASA CR OR TMX OR AD NUMBER)

(CODE) 15
(CATEGORY)

FACILITY FORM 602

RESEARCH AND DEVELOPMENT OF MAGNESIUM/ALUMINUM ELECTROFORMING PROCESS FOR SOLAR CONCENTRATORS

By K. Lui, R. Guidotti, and M. Klein

NATIONAL AERONAUTICS AND SPACE ADMINISTRATION

CONTENTS

iii

ILLUSTRATIONS

iv

TABLES

RESEARCH AND DEVELOPMENT OF MAGNESIUM/ALUMINUM
ELECTROFORMING PROCESS FOR SOLAR CONCENTRATORS

By K. Lui, R. Guidotti, and M. Klein
Electro-Optical Systems, Inc.

SUMMARY

Electroformed magnesium aluminum and hardened aluminum are attractive
for use in various space structure applications such as solar concen-
trators, microwave antennas and lightweight solar panels. The program
was undertaken to optimize plating bath characteristics and to develop
a practical plating system. The electroplating and electroforming
studies were based on the use of organic solvents in the ether family
requiring nonaqueous inert gas atmosphere plating conditions.

Bath composition studies were conducted on solvent-solute combinations
to improve conductivity, to reduce bath vapor pressure, to reduce tree
formation during plating, and to improve the structural characteristics
of the deposited material. Electrode studies were conducted to deter-
mine the effects of current density and reverse cycle plating and to
evaluate anode electrochemical reversibility. Physical property mea-
surements were made of electrodeposited layers to determine yield
strength, ultimate strength, moduli of elasticity, and hardness.
Selected samples were chemically analyzed, and metallographic photo-
graphs were made of them. Pilot electroplating equipment was assembled
and 10 x 15 cm flat plate samples in aluminum, hardened aluminum, and
magnesium were fabricated. In addition, a 30.5-cm paraboloid mirror
was electroformed out of aluminum.

Based on the results of the programs it was found that changes in the
aluminum-ether plating bath composition can result in deposits that
have different grain structures and, therefore, different mechanical
properties. A mixed ether-aluminum bath was developed that results in

a deposit that has a yield strength of approximately 2-1/2 times that of the soft aluminum. This mixed ether bath also has a higher boiling point than the Brenner bath which reduces both evaporation and hazard. Attempts to deposit aluminum alloys to improve the mechanical characteristics have not been successful to date but offer the potential of additional improvements.

Prior to this program, Electro-Optical Systems had developed a proprietary magnesium plating bath, and some of the investigations of the program included the optimization of this bath and the evaluation of a mixed Al-Mg bath. The Al-Mg bath yielded a pure aluminum deposit with no codeposition of magnesium. However, the aluminum had mechanical characteristics (17,000 yield) between that of the Brenner bath (8500 yield) and that of the mixed ether bath (23,000 yield). The grain structure of the aluminum deposit was changed, apparently by changes in the electrode polarization due to the mixed bath. The magnesium bath was further perfected by the slow addition of alkyl halide during the plating process to retard dendrite formation. This enables the deposition of layers approximately 0.25 mm thick which are relatively clean.

With the improvements derived and experience obtained from this program, the electrodeposition of useful structures of aluminum and magnesium has been considerably advanced. The familiarity gained by working with the nonaqueous organic solvents provides confidence that these baths can be reduced to practice on a routine basis. However, additional work is needed to obtain a better understanding of reaction mechanisms and controlling variables and to further improve the mechanical properties of the electrodeposits.

2

INTRODUCTION

This final report presents the progress made on the research and development of magnesium-aluminum electroforming processes for solar concentrators under NASA Contract NAS1-6218 for the period 13 May 1966 through 10 May 1967. Electroformed magnesium and magnesium-aluminum (hardened aluminum) are attractive for use in various space structure applications such as solar concentrators, microwave antennas, and lightweight solar panels. To benefit from the potential high replication and lightweight possibilities of these processes, studies to optimize plating bath characteristics and to develop a practical plating system were conducted. The program was divided into three main areas: Electrotechnology Studies, Process Development, and Electroforming Studies. Appendix A is an outline of the Statement of Work for the program.

To electrodeposit aluminum or magnesium, it is necessary to employ a nonaqueous plating bath. The work conducted during this program concentrated on the use of organic solvents in the ether family. Work conducted in this area prior to this program had demonstrated the ability to electroplate aluminum from a Brenner bath (diethylether-$AlCl_3$-$LiAlH_4$).[1,2] However, the form of aluminum obtained was dead soft with low strength characteristics.

By studying electrode processes and the use of additives in the plating bath, it was hoped that the bath characteristics could be optimized and the mechanical properties of the electrodeposit improved as a result. To demonstrate the practicability of the baths so developed, flat-plate samples and a paraboloid mirror were to be electroformed,

1. D. E. Couch and A. Brenner, J. Electrochem. Soc. 99, 234 (1952)
2. J. H. Connor and A. Brenner, J. Electrochem. Soc. 103, 657 (1956)

TECHNICAL, DISCUSSION

Electrotechnological Studies

Experimental apparatus in controlled environment. - Preparation and operation of the magnesium and aluminum plating baths is very hazardous due to the ether content, plus the fact that the bath reacts with oxygen, moisture, and carbon dioxide. Therefore, all experiments were performed in a dry nitrogen atmosphere within a glove box. Two commercial dry boxes were modified to include a cooling coil which can be immersed in the plating bath and a centralized control panel mounted within easy reach of the worker so that he can operate the filtering systems, the purge lines, the power supply, and the circulating drying train pump without taking both hands out of the glove box. One of the two operating units is shown in Fig. 1. A third glove box is shown in Fig. 2. This unit is double faced; that is, handling of work can be done from two sides, with 1-1/2 times more enclosed area for the placement of larger plating cells.

Materials were inserted or removed from the glove box through the antechamber connected to the glove box. Materials were placed in the chamber, which was flushed for 1/2 hour with dry nitrogen (while simultaneously under vacuum) before the materials were transferred into the glove box. The exhaust gases from the vacuum pump were vented directly to a hood.
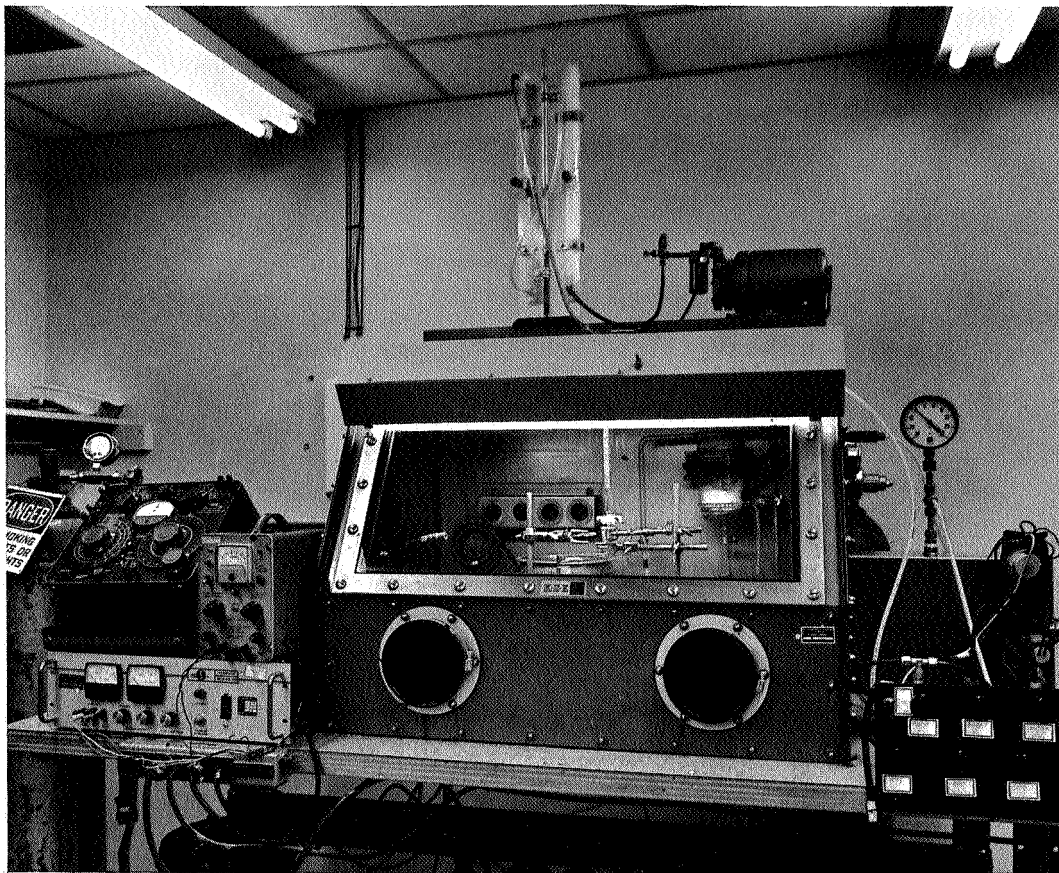
Figure 1. Modified Glove Box for Controlled Mg-Al Electrodeposition
Experiment

5
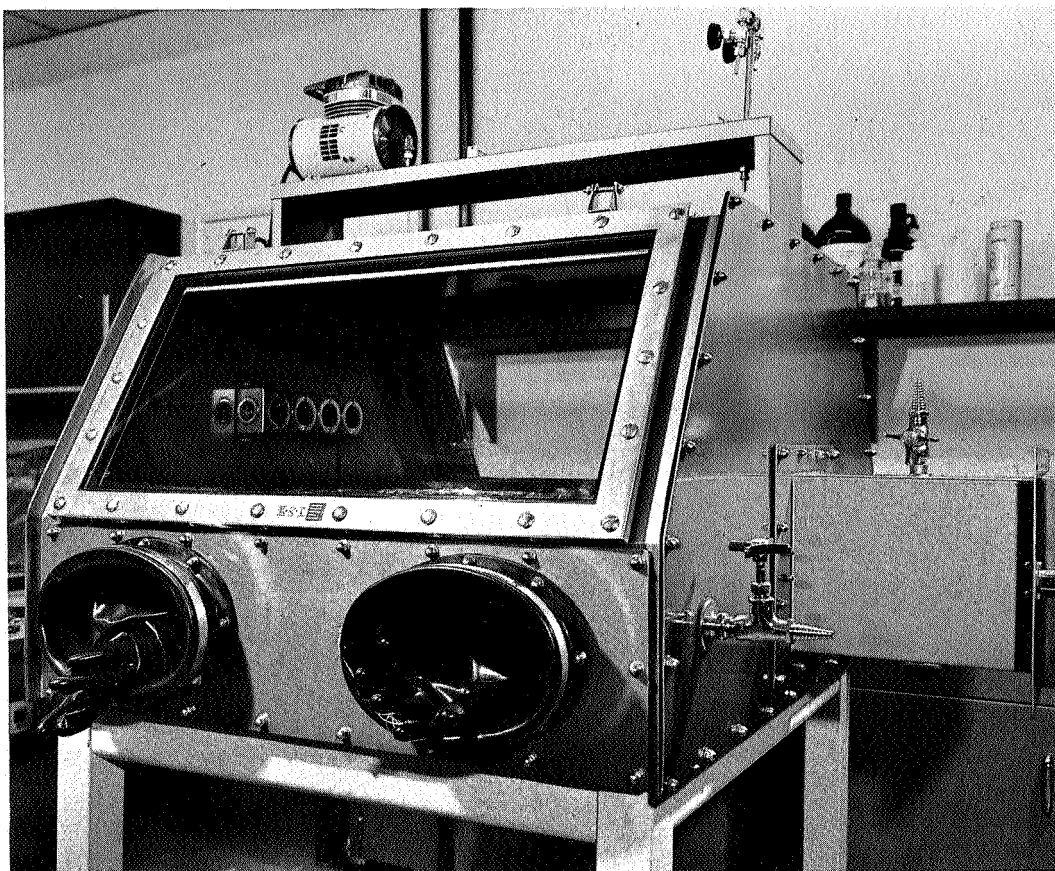
Figure 2.   Two–Face Glove **Box** for Enclosing Larger Plating Cells

6

Magnesium Plating

Conductivity tests: The present Grignard magnesium bath solution possesses relatively low conductance as a plating medium. As poor conductivity results in poor energy efficiency, salt additives were tested in an attempt to improve the solution conductivity.

Conductivity tests were carried out in *a* glove box under a dry nitrogen atmosphere. Measurements were made in a calibrated conductivity cell with a cell constant of 10.2. Cell impedance was measured using an impedance bridge. Conductivity values were gathered for 1 gram of additive salt to $10^{-4}m^3$ (100 ml) of magnesium plating solution at $298^{\circ} \pm 0.5^{\circ}K$ ($25^{\circ} \pm 0.5^{\circ}C$). The results are given in Table **I**.

Inspection of this table reveals that the increase, if any, in conductivity caused by salt addition is very low. In most cases, the conductivity dropped slightly. Only two salts, magnesium chloride and tetraethylammonium bromide, caused an increase in conductivity at the $1 g/10^{-4}m^3$ (1.0 g/100 ml) level. These two salts were then added in **250** mg portions to saturation level [$5 g/10^{-4}m^3$ (5 g/100 ml) for tetraethylammonium bromide and $3 g/10^{-4}m^3$ (3 g/100 ml) for $MgCl_2$]. There were no significant improvements in conductivity with larger quantities.

Electrodeposition tests: Electrodeposition tests with the $MgCl_2$-saturated magnesium plating solution yielded a very spongy deposit as compared with the fairly coherent deposit from a normal magnesium plating solution. An electrodeposition test with the magnesium plating solution saturated with tetraethylammonium bromide yielded a deposit no different than that from a normal magnesium plating solution.

TABLE I

CONDUCTIVITY OF MAGNESIUM BATH SOLUTION WITH ADDITIVES

AT 1 g/10^{-4} m^3 (1 g/100 ml) OF BATH SOLUTION

Additive			Conductivity ohm^{-1} cm^{-1} at 298° ±0 5°K
Magnesium bath solution			8.15×10^{-4}
Magnesium perchlorate			7.55×10^{-4}
Magnesium chloride			8.45×10^{-4}
Magnesium oxide			7.85×10^{-4}
Magnesium acetate			7.50×10^{-4}
Magnesium fluoride			5.10×10^{-4}
Magnesium iodide			7.85×10^{-4}
Sodium iodide			2.30×10^{-5}
Tetraethylammonium chloride			1.17×10^{-4}
Tetraethylammonium bromide			9.25×10^{-4}
Tetraethyl ammonium iodide			2.55×10^{-5}
Lithium borohydride			2.33×10^{-5}
Lithium aluminum hydride			Solution coagulated – no test
Tetraethylammonium bromide	5 gm	10 minutes	8.8×10^{-4} T.E.A. bromide did not all dissolve
Tetraethylammonium bromide	5 gm	60 minutes	7.34×10^{-4}
Tetraethylammonium bromide	5 gm	120 minutes	9.25×10^{-4}
Magnesium chloride	3 gm	120 minutes	8.5×10^{-4}

8

Addition of reactive chemical species - alkyl halides: Electro-deposition of magnesium from a Grignard solution yields very spongy noncoherent deposits. It has been found that slow addition of an alkyl halide causes the sponge to disappear, and a relatively thicker coherent deposit can be obtained. A plating cell was assembled whereby continuous addition of an alkyl halide solution could·be controlled. Several alkyl halides, such as methyl iodide, ethyl iodide, ethyl bromide, butyl iodide, and butyl bromide were tested. Ethyl bromide was found to be most effective in retarding sponge and dendrite formation. The technique is to add ethyl bromide at a rate which yields a concentration sufficient to retard the formation of sponge and dendrites but insufficient to chemically corrode the deposit on the electrode. The criteria used to determine the optimum rate of ethyl bromide addition are cathode current efficiency and the appear-ance of the resultant deposit. Table II is a summary of the experi-mental tests. A plot of current efficiency versus rate of ethyl bromide addition was made to determine the optimum rate. The optimum rate in terms of current efficiency (Fig. 3) appeared to be 0.030 mole of ethyl bromide per hour. (By use of an automatic fluid injector later in the study, the alkyl halide additions were very accurately controlled and the quantity of alkyl halide required was more accurately found to be 15% of the total ampere equivalence.) When referred to tests where the addition of ethyl bromide was 0.027 to 0.035 mole/hour, the appearance of the deposits was light gray with very little surface defects. Thus, ethyl bromide addition at 0.030 mole/hour fulfilled both criteria set for optimum addition rate. This rate, however, only applies to one set of plating conditions, where the conditions are:

Current density	10.8 mA/cm^2
Electrode size	25.8 cm^2
Electrolyte geometry	$5 \times 10^{-4} m^3$ (500 ml)

TABLE III

SUMMARY OF ADDITION OF ETHYL BROMIDE DURING ELECTRODEPOSITION

Run No.	Duration of Electrodeposition (hr)	Ethyl Bromide Added				Current Efficiency (%)	Appearance of Deposit
		Concentration	Total Volume (x $10^{-6} m^3$)	Total Moles	Rate mole/hr		
1	4	100%	32.5	0.426	0.106	--	Most of the deposit was corroded by the EB
2	8	100%	48.6	0.636	0.080	--	Most of the deposit was corroded by the EB
3	6	100%	24.0	0.314	0.052	77	Light gray, and a few pits
4	2	50% EB, 50% diethyl ether	8.0	0.053	0.027	79	Light gray, slightly nodular, very few trees on edges
5	2	EB:THF (1:2)	8.0	0.035		54	Darker gray; coarse at spots
6	2	0	0	0	0	51.1	Light gray, trees at edges
7	3	50% EB, 50% ether	3.0	0.039	0.013	63	Light gray, no pits; rough at spots
8	--	100%	--	--	--	--	Not completed
9	8	EB & THF 1:1	8.0	0.053	0.027	67	Metallic deposit gray
10	8	100%	8.0	0.053	0.027	79	Light gray, metallic
11	30	100%	18.0	0.235	0.786	70	Light gray, spotted
12	5	100%	4.0	0.052	0.015	23.4	Light gray, few trees
13	--	--	--	--	--	--	Sol contamination
14	7	100%	5.6	0.073	0.014	23.1	Mg dissolved by EB
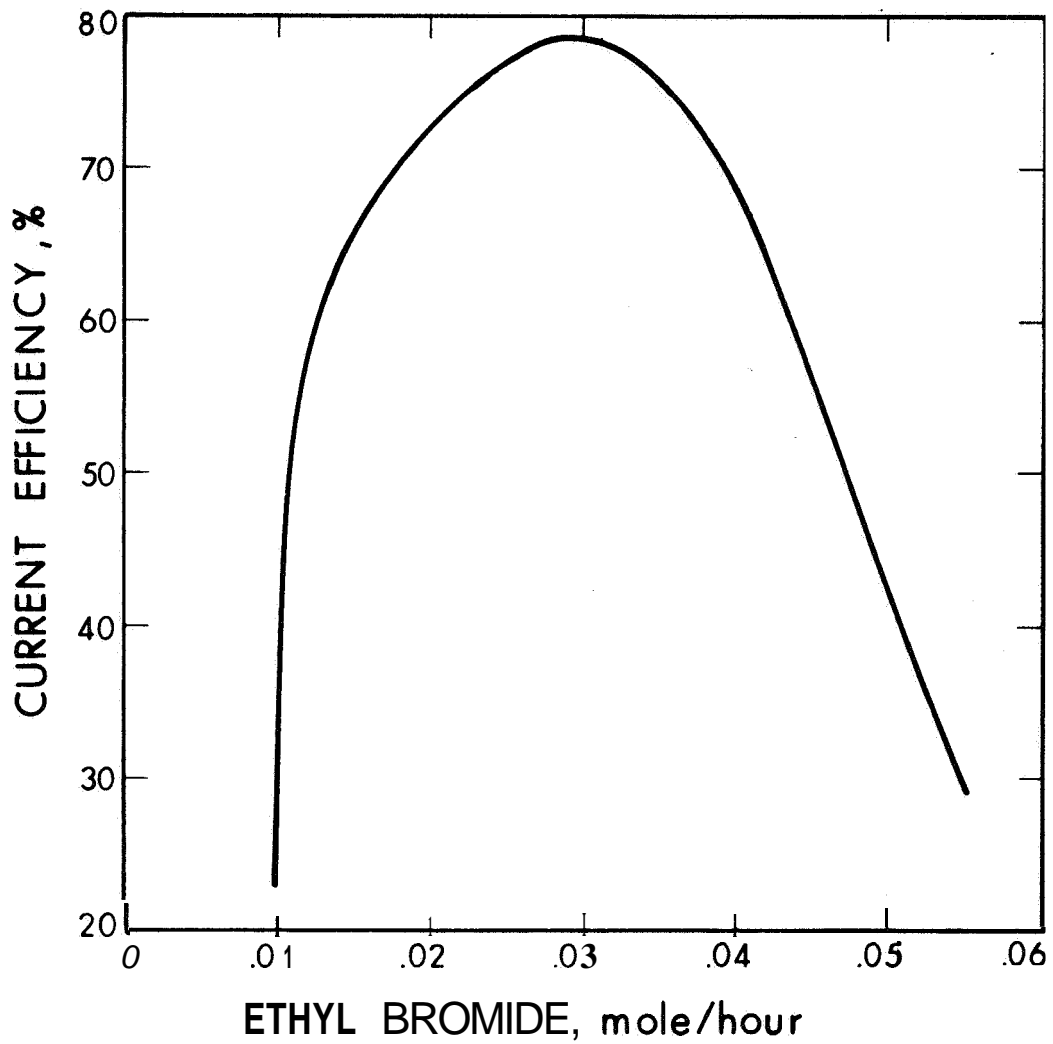
Figure 3. Current Efficiency versus Rate of Ethyl Bromide Additions

For another set of plating conditions, the optimum rate will be different. However, there should be a common proportionality factor and this could be determined by ascertaining the optimum rate at two or more sets of plating conditions.

Aluminum plating.

Solution preparation: Care must be exercised in the preparation of the $AlCl_3$–diethyl ether solution because a considerable amount of heat is generated during the process. It is necessary to cool the ether during addition of anhydrous $AlCl_3$,   This is done by use of an immersion cooling coil through which a coolant is circulated. Stirring is effected by use of a large magnetic stirrer. The $AlCl_3$ should be slowly stirred into the cold ether so that the bath temperature does not rise above $303^{O}K$ during addition. With too rapid addition of $AlCl_3$, severe localized heating occurs, and the solution darkens in color from a light amber to an orange–red. It has been found that deposits plated from the darkened solution are not always satisfactory.

After $AlCl_3$ addition has been completed, it is advisable to allow the solution to remain undisturbed overnight to permit the minute gray suspended particles to settle out. The solution then can be readily filtered through a medium porosity fritted–glass Buchner. (A coarse porosity Buchner does not always remove all of the small suspended particles.)   After filtering, the solution should be crystal clear and a light amber in color.

Cooling is not required in the preparation of $LiAlH_4$–diethyl ether solutions. A considerable amount of insoluble light gray material remains after addition of the $LiAlH_3$ to the ether. A large

12

part of this settles out upon standing, if the solution has not been made too concentrated. When the solution contains 100 g of $LiAlH_4$ or less per $10^{-3}m^3$ (1), a large part of the gray matter settles out. However, if more than 250 g of $LiAlH_4$ is added per $10^{-3}m^3$ (1) of solution, this gray matter tends to remain suspended in solution which makes filtering more difficult. The best filtering technique is to use a coarse fritted-glass Buchner with fine spun glass as a prefilter to prevent rapid clogging. A stainless steel screen clamped on top of the spun glass to prevent the prefilter from lifting off the fritted glass is recommended. After preparation of the filtered $LiAlH_4$ solution, it should be stored in closed containers under an inert atmosphere (e.g., the glove box) prior to its use.

The aluminum plating solution is prepared by mixing together the $AlCl_3$ and the $LiAlH_4$ solutions. The $LiAlH_4$-ether solution must be added to the $AlCl_3$-ether solution at such a rate as to prevent excessive foaming, to prevent the temperature from rising above 303^oK and, to prevent excessive localized precipitation. The addition of $LiAlH_4$-ether solution is controlled through a separatory funnel. The addition of LiAlH-ether solution is completed when the concentration is between 0.4 and 0.5M in the resultant solution. The concentration of $AlCl_3$ in the resultant solution is 3.4M.

Lowering the aluminum bath vapor pressure: Evaporation losses of the bath solution can be reduced by decreasing the bath vapor pressure. This can be brought about by adding solvents with higher boiling points to the ether bath. The additive solvents must possess the following characteristics:

- Chemically inert to the bath constituents.
- Completely miscible.

- High boiling point (a substantial rise in bath boiling point can be realized by a relatively small addition).
- No adverse effects on the mode of electrodeposition.
- No lowering of quality of the deposit.

The additive solvents studied were: butyl ether $(bp=415^{\circ}K)$; hexyl ether $(bp=370^{\circ}K/9 \times 10^{-3}m)$; anisole $(bp=425^{\circ}-427^{\circ}K)$; 1,2-dimethoxyethane $(bp=356^{\circ}-358^{\circ}K)$; bis (2-methoxyethoxy ethyl) ether $(bp=393^{\circ}-395^{\circ}K/3 \times 10^{-3}m)$; bis (2-chloroethyl) ether $(bp=449^{\circ}-451^{\circ}K)$; and bis (2-butoxyethyl) ether $(bp=513^{\circ}K)$.

The solvent ratio and the resultant boiling point at the concentration of 3 molar $AlCl_3$ and the appearance of the electrodeposit are given in Table III. Other solvent ratios which could not maintain a 3 molar concentration in $AlCl_3$ are not shown in the table. The boiling point of the $AlCl_3$ bath was elevated anywhere from 283° to $383^{\circ}K$. Only two of the higher boiling-point baths yielded deposits comparable to the normal diethyl ether bath. These are diethyl ether: anisole $(2:1, bp=367^{\circ}K)$ and diethyl ether: bis (2 chloroethyl) ether $(2:1, bp=375^{\circ}K)$ mixtures. These two higher boiling-point plating solutions offer baths with vapor pressures less than half that of the existing bath. This would greatly reduce the health and fire hazards. **Also,** it may be possible to operate the bath in a partially open tank with a heavy inert gas blanket instead of in a completely enclosed tank. This would greatly expedite the handling of work to and from the bath.

TABLE III

BOILING POINT ELEVATION BY THE ADDITION
OF HIGHER BOILING POINT ETHERS
$AlCl_3$ = 3 Molar

Ratio of Ether to Additive Ether	Higher Boiling Ether	Boiling Point (^{o}K)	Appearance of Deposit
1:0	Bis(2-butoxyethyl)2 ether	315	Good, white, ductile
4:1	Bis(2-butoxyethyl) ether	323	Good, white, ductile
4:1	Butyl ether	335	Dark, straited, brittle
1:1	Butyl ether	371	Dark, straited, brittle
2:1	Anisole	367	Good, slightly gray, ductile
4:1	Hexyl ether	332-333	Dark, straited, brittle
2:1	Hexyl ether	351-354	Dark, straited, brittle
1:1	Hexyl ether	276	Dark, straited, brittle
4:1	Bis(2-chloroethyl) ether	333-335	Gray, coherent, brittle
2:1	Bis(2-chloroethyl) ether	373-374	Good, coherent, ductile
1:1	Bis(2-chloroethyl) ether	437-439	Light green, coherent, brittle

15

The effect of the atmosphere on the bath solution: It is known
that the magnesium and the aluminum bath solutions are decomposed
by oxygen, CO_2, and moisture. However, no quantitative data are
available to show the rate of the degree of decomposition. Experi-
ments were performed in an attempt to measure the duration frequency
of exposing the bath solution to the atmosphere. The four types of
bath solutions tested were: (1) normal aluminum plating bath,
(2) magnesium plating bath, *(3)* magnesium-aluminum bath, and
(4) ethyl magnesium bromide-tetrahydrofuran solution. Sixteen test
samples were used for each bath solution. Each sample was properly
identified and was assigned an exposure duration frequency schedule;
e.g., the sample labeled ALTG-A-1 signifies a magnesium-aluminum
bath solution exposed daily to the atmosphere for 10 seconds.

The conductivity of the sample was taken after each exposure.
The sample was exposed by opening the sealed container and pouring
the solution into a beaker, then back into the container where the
exposure time was completed. The bottle was then purged with
nitrogen before it was resealed. Electrodeposition tests on
representative samples were made and the appearance of the resultant
deposit was noted. (These results are given in Table IV.) The
results indicated that all the bath solutions have greater tolerance
for air and moisture than expected. Frequent short exposures (15
seconds to 1 minute daily) have no ill effect on electrodeposits.
However, solutions exposed for long durations *(30* minutes) either
yielded poor plates or completely decomposed solutions.

Electrode studies. - The electrode study was intended to
resolve problems in optimizing quantities, such as cathode current
efficiency, anode current efficiency, grain structure, rate of
deposition (current density), and thickness of deposit. The

TABLE IV

SUMMARY OF RESULTS OF DURATION-FREQUENCY EXPOSURE OF MAGNESIUM-ALUMINUM PLATING SOLUTIONS

I Solution No.	II Conductivity Before Exposure (ohm⁻¹ cm⁻¹)	III Lowest Conductivity (ohm⁻¹ cm⁻¹)	IV No. of Exposures at III	V Final Conductivity (ohm⁻¹ cm⁻¹)	VI Total Exposures	VII Cathode Current Efficiency	VIII Appearance of Plate
AL-A-1*	7.05×10^{-3}	$5\ 84 \times 10^{-3}$	10 sec 16 times	$5\ 84 \times 10^{-3}$	10 sec 16 times	100 3%	Smooth center; very rough around edges
AL-A-2	7.05×10^{-3}	$6\ 0 \times 10^{-3}$	10 sec 7 times	$6\ 0 \times 10^{-3}$	10 sec 16 times		
AL-A-3	7.05×10^{-3}	$6\ 18 \times 10^{-3}$	10 sec 3 times	$6\ 18 \times 10^{-3}$	10 sec 16 times		
AL-A-4	7.05×10^{-3}	8×10^{-3}	10 sec 1 time	8×10^{-3}	10 sec 1 time		
AL-B-1	7.05×10^{-3}	$5\ 8 \times 10^{-3}$	1 min 16 times	$5\ 8 \times 10^{-3}$	1 min 16 times		
AL-B-2	7.05×10^{-3}	$5\ 8 \times 10^{-3}$	1 min 7 times	$5\ 84 \times 10^{-3}$	1 min 7 times	100 2%	Bottom smooth; top rough with trium at edges
AL-B-3	7.05×10^{-3}	$6\ 7 \times 10^{-3}$	1 min 3 times	$6\ 37 \times 10^{-3}$	1 min 3 times		
AL-B-4	7.05×10^{-3}	$6\ 8 \times 10^{-3}$	1 min 1 time	8×10^{-3}	1 min 1 time		
AL-C-1	7.05×10^{-3}	$4\ 8 \times 10^{-3}$	10 min 16 times	$4\ 8 \times 10^{-3}$	10 min 16 times		
AL-C-2	7.05×10^{-3}	$4\ 64 \times 10^{-3}$	10 min 7 times	$4\ 64 \times 10^{-3}$	10 min 7 times		
AL-C-3	7.05×10^{-3}	$5\ 1 \times 10^{-3}$	10 min 3 times	$5\ 1 \times 10^{-3}$	10 min 3 times	100 2%	Very smooth; little growth at edges

7

17

TABLE 3

SUMMARY OF RESULTS OF DURATION-FREQUENCY EXPOSURE OF MAGNESIUM-ALUMINUM PLATING SOLUTIONS (Contd)

I Solution No.	II Conductivity Before Exposure (ohm⁻¹ cm⁻¹)	III Lowest Conductivity (ohm⁻¹ cm⁻¹)	IV No. of Exposures at III	V Final Conductivity (ohm⁻¹ cm⁻¹)	VI Total Exposures	VII Cathode Current Efficiency	VIII Appearance of Plate
AL-C-4	7.05×10^{-3}	6.6×10^{-3}	10 min 1 time	6.6×10^{-3}	10 min 1 time		
AL-D-1	7.05×10^{-3}	4.45×10^{-3}	30 min 11 times	7.3×10^{-3}	30 min 16 times		
AL-D-Z	7.05×10^{-3}	5.38×10^{-3}	30 min 4 times	5.38×10^{-3}	30 min 4 times		
AL-D-3	7.05×10^{-3}	5×10^{-3}	30 min 4 times	5.7×10^{-3}	30 min 4 times		
AL-D-4	7.05×10^{-3}	4×10^{-3}	30 min 1 time	4×10^{-3}	30 min 1 time	100.4%	Bottom 1/3 very smooth; top 2/3 smooth with little growth
4-A-1	7.05×10^{-3}	5.53×10^{-3}	10 sec 15 times	5.53×10^{-3}	10 sec 16 times		
4-A-2	7.05×10^{-3}	8×10^{-3}	10 sec 4 times	5.83×10^{-3}	10 sec 4 times	100.2%	smooth; little growth on edges
AL-G-A-3	7.05×10^{-3}	$5.a7 \times 10^{-3}$	10 sec 3 times	$5.a7 \times 10^{-3}$	10 sec 3 times		
AL-G-A-4	7.05×10^{-3}	8×10^{-3}	10 sec 1 time	6.8×10^{-3}	10 sec 1 time		
4-a-1	7.05×10^{-3}	37×10^{-3}	1 min 13 times	5.37×10^{-3}	1 min 16 times		

TABLE IV

SUMMARY OF RESULTS OF DURATION-FREQUENCY EXPOSURE OF MAGNESIUM-ALUMINUM PLATING SOLUTIONS (Contd)

I Solution No.	II Conductivity Before Exposure (ohm^{-1} cm^{-1})	III Lowest Conductivity (ohm^{-1} cm^{-1})	IV No. of Exposures at III	V Final Conductivity (ohm^{-1} cm^{-1})	VI Total Exposures	VII Cathode Current Efficiency	VIII Appearance of Plate
AL-G-B-2	7 05 x 10^{-3}	5 83 x 10^{-3}	1 min 3 times	5 83 x 10^{-3}	1 min 3 times	100.4%	Smooth; little growth around edges
AL-G-B-3	7 05 x 10^{-3}	5 53 x 10^{-3}	1 min 3 times	5 53 x 10^{-3}	1 min 3 times		
AL-G-B-4	7 05 x 10^{-3}	6 59 x 10^{-3}	1 min 1 time	6 59 x 10^{-3}	1 min 1 time		
AL-G-C-1	7 05 x 10^{-3}	4 08 x 10^{-3}	10 min 15 times	4 08 x 10^{-3}	10 min 16 times		
AL-G-C-2	7 05 x 10^{-3}	4 25 x 10^{-3}	10 min 7 times	4 25 x 10^{-3}	10 min 7 times		
AL-G-C-3	5 x 10^{-3}	4 68 x 10^{-3}	10 min 1 time	4 68 x 10^{-3}	10 min 1 time	100 3%	Smooth; lots of growth around edges
AL-G-C-4	7 05 x 10^{-3}	6 0 x 10^{-3}	10 min 1 time	6 0 x 10^{-3}	10 min 1 time		
AL-G-D-1	7 05 x 10^{-3}	4 08 x 10^{-3}	30 min 10 times	6 0 x 10^{-3}	30 min 10 times		
AL-G-D-2	5 x 10^{-3}	4 25 x 10^{-3}	30 min 7 times	4 25 x 10^{-3}	30 min 7 times		
AL-G-D-3	7 08 x 10^{-3}	4 44 x 10^{-3}	30 min 3 times	4.44 x 10^{-3}	30 min 3 times		

TABLE IV

SUMMARY OF RESULTS OF DURATION-FREQUENCY EXPOSURE OF MAGNESIUM-ALUMINUM PLATING SOLUTIONS (Contd)

I Solution No.	II Conductivity Before Exposure $(\text{ohm}^{-1}\,\text{cm}^{-1})$	III Lowest Conductivity $(\text{ohm}^{-1}\,\text{cm}^{-1})$	IV No. of Exposures at III	V Final Conductivity $(\text{ohm}^{-1}\,\text{cm}^{-1})$	VI Total Exposures	VII Cathode Current Efficiency	VIII Appearance of Plate
AL-G-D-4	7.05×10^{-3}	5.1×10^{-3}	30 min 1 time	5.1×10^{-3}	30 min 1 time	100.4%	Smooth; grainy at top; little growth at edges
AL-T-A-1	7.75×10^{-3}	5.1×10^{-3}	10 sec 15 times	5.1×10^{-3}	10 sec 16 times	100.5%	Very smooth; no growth at edges
AL-T-A-2	7.75×10^{-3}	5.84×10^{-3}	10 sec 7 times	5.84×10^{-3}	10 sec 6 times		
AL-T-A-3	7.75×10^{-3}	5.67×10^{-3}	10 sec 3 times	5.67×10^{-3}	10 sec 3 times		
AL-T-A-4	7.75×10^{-3}	6.8×10^{-3}	10 sec 1 time	6.8×10^{-3}	10 sec 1 time		
AL-T-B-1	7.75×10^{-3}	5.1×10^{-3}	1 min 14 times	5.37×10^{-3}	1 min 16 times		
AL-T-B-2	7.75×10^{-3}	5.23×10^{-3}	1 min 7 times	5.23×10^{-3}	1 min 7 times	100.5%	Very smooth; slight growth at bottom edge
AL-T-B-3	7.75×10^{-3}	5.5×10^{-3}	1 min 3 times	5.5×10^{-3}	1 min 3 times		
AL-T-B-4	7.75×10^{-3}	6.8×10^{-3}	1 min 1 time	6.8×10^{-3}	1 min 1 time		
AL-T-C-1	7.75×10^{-3}	3.78×10^{-3}	10 min 16 times	3.78×10^{-3}	10 min 6 times		
AL-T-C-2	7.75×10^{-3}	4.85×10^{-3}	10 min 7 times	4.85×10^{-3}	10 min 7 times		

TABLE IV

SUMMARY OF RESULTS OF DURATION-FREQUENCY EXPOSURE OF MAGNESIUM-ALUMINUM PLATING SOLUTIONS (Contd)

I Solution No.	II Conductivity Before Exposure ($ohm^{-1} cm^{-1}$)	III Lowest Conductivity ($ohm^{-1} cm^{-1}$)	IV No. of Exposures at III	V Final Conductivity ($ohm^{-1} cm^{-1}$)	VI Total Exposures	VII Cathode Current Efficiency	VIII Appearance of Plate
AL-T-C-3	7.75×10^{-3}	5.1×10^{-2}	10 min 3 times	5.1×10^{-3}	10 min m times	100 a%	Very smooth; slight growth on edges
AL-T-C-4	7.75×10^{-3}	$a.8 \times 10^{-3}$	10 min 1 time	6.8×10^{-3}	10 min 1 time		
AL-T-D-1	7.75×10^{-3}	$4.0a3 \times 10^{-3}$	30 min 11 times	6.37×10^{-3}	30 min 16 times		
AL-T-D-2	7.75×10^{-3}	$4.4a \times 10^{-3}$	30 min 7 times	4.64×10^{-3}	30 min b times		
AL-T-D-3	7.75×10^{-3}	$4.a4 \times 10^{-3}$	30 min 3 times	4.64×10^{-3}	30 min m times		
AL-T-D-4	7.75×10^{-3}	$h.a \times 10^{-3}$	30 min 1 time	5.66×10^{-3}	30 min 1 time	None[a]	None - did not plate
AL-TG-A-1	7.4×10^{-3}	4.25×10^{-3}	10 sec 15 times	4.25×10^{-3}	10 sec 16 times	—	Fairly smooth; rough near top; growth at end edges
AL-TG-A-2	7.4×10^{-3}	4.64×10^{-3}	10 sec 7 times	4.64×10^{-3}	10 sec b times		
AL-TG-A-3	7.4×10^{-3}	5.1×10^{-3}	10 sec 3 times	5.1×10^{-3}	10 sec m times		
AL-TG-A-4	7.4×10^{-3}	$a3.a \times 10^{-3}$	10 sec 1 time	6.68×10^{-3}	10 sec 1 time		

TABLE IV

SUMMARY OF RESULTS OF DURATION-FREQUENCY EXPOSURE OF MAGNESIUM-ALUMINUM PLATING SOLUTIONS (Contd)

I Solution No.	II Conductivity Before Exposure (ohm⁻¹ cm⁻¹)	III Lowest Conductivity (ohm⁻¹ cm⁻¹)	IV No. of Exposures at III	V Final Conductivity (ohm⁻¹ cm⁻¹)	VI Total Exposures	VII Cathode Current Efficiency	VIII Appearance of Plate
AL-TG-B-1	$7\ 4 \times 10^{-3}$	4.34×10^{-3}	1 min 15 times	$4\ 4 \times 10^{-3}$	1 min 16 times	83.5%	Smooth; very little growth around edges
AL-TG-B-2	$7\ 4 \times 10^{-3}$	$4.a3 \times 10^{-3}$	1 min 7 times	$5\ 6 \times 10^{-3}$	1 min 7 times		
AL-TG-a-3	$7\ 4 \times 10^{-3}$	4.86×10^{-3}	1 min 3 times	$4\ 8a \times 10^{-3}$	1 min 7 times		
AL-TG-a-4	$7\ 4 \times 10^{-3}$	6.37×10^{-3}	1 min 1 time	$6\ m \times 10^{-3}$	1 min 1 time		
AL-TG-C-1	$7\ 4 \times 10^{-3}$	3.52×10^{-3}	10 sec 15 times	$4\ 25 \times 10^{-3}$	10 sec 16 times		
AL-TG-C-2	$7\ 4 \times 10^{-3}$	3.7×10^{-3}	10 min 7 times	$3\ 78 \times 10^{-3}$	10 min 7 times		
AL-TG-C-3	$7\ 4 \times 10^{-3}$	$4.z5 \times 10^{-3}$	10 min 3 times	$4\ 25 \times 10^{-3}$	10 min 3 times		
AL-TG-C-4	$7\ 4 \times 10^{-3}$	6.0×10^{-3}	10 min 1 time	$6\ 0 \times 10^{-3}$	10 min 1 time	100 4%	Smooth; little growth around edges
AL-TG-4-1	$7\ 4 \times 10^{-3}$	3.84×10^{-3}	30 min 11 times	$5\ 38 \times 10^{-3}$	30 min 16 times		
AL-TG-4-2	$7\ 4 \times 10^{-3}$	4.25×10^{-3}	30 min 7 times	$4\ 25 \times 10^{-3}$	30 min 7 times		

TABLE IV

SUMMARY OF RESULTS OF DURATION-FREQUENCY EXPOSURE OF MAGNESIUM-ALUMINUM PLATING SOLUTIONS (Contd)

I Solution No.	II Conductivity Before Exposure $(ohm^{-1} cm^{-1})$	III Lowest Conductivity $(ohm^{-1} cm^{-1})$	IV No. of Exposures at III	V Final Conductivity $(ohm^{-1} cm^{-1})$	VI Total Exposures	VII Cathode Current Efficiency	VIII Appearance of Plate
AL-TG-D-3	$7\ 4 \times 10^{-3}$	$m\ 92 \times 10$	30 min m times	3.92×10^{-3}	30 min m times		
AL-TG-D-4	$7\ 4 \times 10^{-3}$	$4\ 86 \times 10^{-3}$	30 min 1 time	4.86×10^{-3}	30 min 1 time	99.8%	Very smooth; no growth around edges

*AL — 3-molar solution $AlCl_3$ in ethyl ether
AL-T — 3-molar solution $AlCl_3$ in ethyl ether plus $2\ 5 \times 10^{-4}\ E^3$ (250 ml)
AL-G — Modified Al Bath Solution
AL-TG — Mg/Al Bath Solution

A — exposed 10 sec each time   1 — opened once every day
B — exposed 1 min each time   2 — opened twice a week
C — exposed 10 min each time   3 — opened once a week
D — exposed 30 min each time   4 — opened once every 4 weeks

parameters which could govern the attainment of the aforementioned entities were investigated.

The effect of current density: High current density in electrodeposition is desirable because the rate thickness buildup is in direct proportion to the current density. In addition, the electrodeposit crystal structure becomes increasingly finer with the increase in current density. At too high current densities, however, burning of the deposit normally occurs, accompanied by the excessive formation of dendrites at the corner and edges of the work piece. A study was made to determine the operable current density range for the magnesium and magnesium/aluminum bath. The results of this study are summarized in Table V.

The effect of periodic reverse-cycling: It has been reported by other workers that periodic reverse-cycling produces deposits that are relatively free of nodules and other imperfections normally encountered with straight dc. It has been observed that nodules and roughness become more noticeable at high current densities and in thickness buildups greater than 0.38 mm. Thus, by the use of periodic reverse-cycling, it is possible to operate at higher current density and to build up a greater plate thickness prior to the advance of nodule formation. Tests were conducted to evaluate this effect with forward-to-reverse ratios in the range of 3:1 to 60:1 with the magnesium plating solution. It was observed that the deposit became visibly more porous at ratios greater than 12:1; nodule formation was comparable to straight dc plating at ratios lower than 26:1 when operated at a current density of $10.8mA/cm^2$. The optimum forward-to-reverse ratio appeared to be near 20:1 (i.e., 180 seconds plating and 9 seconds deplating).

TABLE V

EFFECT OF CURRENT DENSITY FOR THE ELECTRODEPOSITION OF MAGNESIUM AND MAGNESIUM–ALUMINUM

Plating Bath	Current Density (mA/cm^2)	Cell Voltage (V)	Appearances of Deposit
Magnesium	2	2.5	Coarse crystalline; porous, light gray
	5	6.0	Coarse crystalline, light gray, less porous than at 2 mA/cm^2
	10	8.6	Light gray, smooth, a few trees at the edges
	20	10.2	Light gray, smooth, more trees at the edges than at 10 mA/cm^2
	40	15.5	Gray, numerous trees all over
Magnesium–Aluminum	2	0.6	White, noticeable voids, non-adherent near the center
	5	1.3	White, some voids and small pits, some peeling
	10	3.3	White, coherent, some pits at the center
	20	7.8	White, smooth, good granular structure
	40	16.2	White, not as smooth as 20 $mA/cm2$, nodular at edges
	60	31.7	White, very granular, trees on edges

The optimum current density for the magnesium bath was between 10 to 15 mA/cm^2 and between 20 to 40 mA/cm^2 for the magnesium–aluminum bath.

25

Periodic reverse cycling can only retard the formation of nodules, but cannot completely eliminate their formation without greatly sacrificing other qualities of the deposit and substantially decreasing the overall plating efficiency.

The electrodissolution of anode materials: In the case of the aluminum bath, an aluminum anode can be electrolytically dissolved at almost 100%. However, even though the aluminum anode is consumed very efficiently, some phenomenon (as yet unexplained) occurs during the plating process that tends to deteriorate the bath. This is evidenced by an increasing bath voltage at a constant current with time. Thus, to maintain the power efficiency and quality of the deposit, more $AlCl_3$ and $LiAlH_4$ must be added periodically. The change in bath characteristics during plating could result from contamination with air or moisture, impurities from the plating equipment, decomposition of the bath solution, contaminants from the anodes, and/or the partial formation of a nonplatable species during the electrodissolution of the anode. Insufficient experimentation was conducted during the program to fully determine the exact cause of the changes in the bath during plating.

Electrodeposition tests with the magnesium plating bath using magnesium anodes revealed that anodic dissolution does not occur. The anodic half cell reaction must then involve other electrolytic reactions with the constituents of the magnesium bath. The most probable reaction is the decomposition of the solvent. Anodic dissolution does take place when aluminum is used, and gold (**1.3** microns) plated on copper is inert.

Chemical means for replenishing the supply of magnesium in solution have been investigated (refer to page 9). The addition of alkyl halides seems to hold the best possibilities at the present time. Tests have shown, however, that the rate of alkyl halide addition and the bulk concentration of these reactants in the bath are very critical and must be maintained within a very narrow range. Time did not permit further refinement of the technique of alkyl halide addition.

Alloying studies: - Thus far, the strengthening of aluminum appears to be a result of grain refinement during metal formation by a probable change in the polarization characteristics. Another possible strengthening technique during metal formation is through alloying by coelectrodeposition. The ability to form alloys by electrodeposition is closely related to the reduction potentials of aluminum or magnesium and various alloying metals. Table VI indicates the reduction potentials as measured in aqueous solutions, of typical metals that are alloyed with aluminum. Metals whose reduction potentials vary considerably, such as magnesium and copper, are extremely difficult to electrodeposit in an alloy condition. Without the modification of the metal ionic form, electrodeposition would result in an almost complete separation of the two metals, with copper (having the lower reduction potential) being deposited first. For codeposition with aluminum, both beryllium and titanium rate first in view of their reduction potentials and, correspondingly, both magnesium and manganese rate second. The practical value of the reduction potentials is that it indicates the decomposition potential which is the reduction potential plus the various polarization potentials. The initial step in an alloying investigation is to measure the decomposition potentials of the magnesium bath. The decomposition potential of an ionic species undergoing electrolysis at an electrode corresponds to the point

TABLE V I

REDUCTION POTENTIALS OF ALUMINUM AND
COMMON ALUMINTJM ALLOYING ELEMENTS

Half Cell Reaction	Reduction Potential (volts)
$Mg \rightarrow Mg^{+2} + 2e^-$	2.34
$Be \rightarrow Be^{+2} + 2e-$	1.85
$Al \rightarrow Al^{+3} + 3e^-$	1.67
$Ti \rightarrow Ti''' + 2e^-$	1.63
$Mn \rightarrow Mn^{+2} + 2e^-$	1.18
$Zn \rightarrow Zn^{+2} + 2e^-$	0.76
$cu \rightarrow Cu^{+2} + 2e^-$	0.34
$H_2 \rightarrow 2H^+ + 2e^-$	0.00

The above is taken at one molar aqueous concentration at one
atmosphere and 298^OK.

of sudden upsurge of the polarization curve. Typical of such curves are the anodic and cathodic polarization curves for the magnesium plating solution (Figs. *4* and 5). The anodic decomposition potential is found to be -1.45V. The cathodic decomposition potential is +0.65V. Both of these voltages are in reference to a platinum wire electrode. (It was observed that Ag-AgCl reference electrode voltages were unstable in the plating solution.)

Figure 6 is a schematic of the cell used for the initial work on decomposition potential measurements. The voltage and current settings were adjusted manually and there were no provisions for precisely controlling the duration of each setting. (Attempts to use a conventional polarograph for the solute screening were unsuccessful since it was observed that the minimum distance required for the dropping mercury electrode arrangement still resulted in too high an IR drop through the organic electrolytes). The present test cell is a modification of the initial test cell. The added auxiliary instruments include a potential controller which scans the current passing through the control electrode between pre-set reference voltage limits. The control electrode can be either the anode or the cathode, depending on the switch position. Two control electrodes are placed in the test electrolyte to provide a fresh electrode surface for either the anodic or cathodic mode. The reference voltage and cell current are recorded on an X-Y recorder.

Figure 7 is the schematic of the polarization curve measurement assembly. With this test assembly, a set of anodic and cathodic polarization curves can be obtained within five minutes. However, before polarization curves are run on prospective candidates for codeposition, they should show a solubility in ether and their
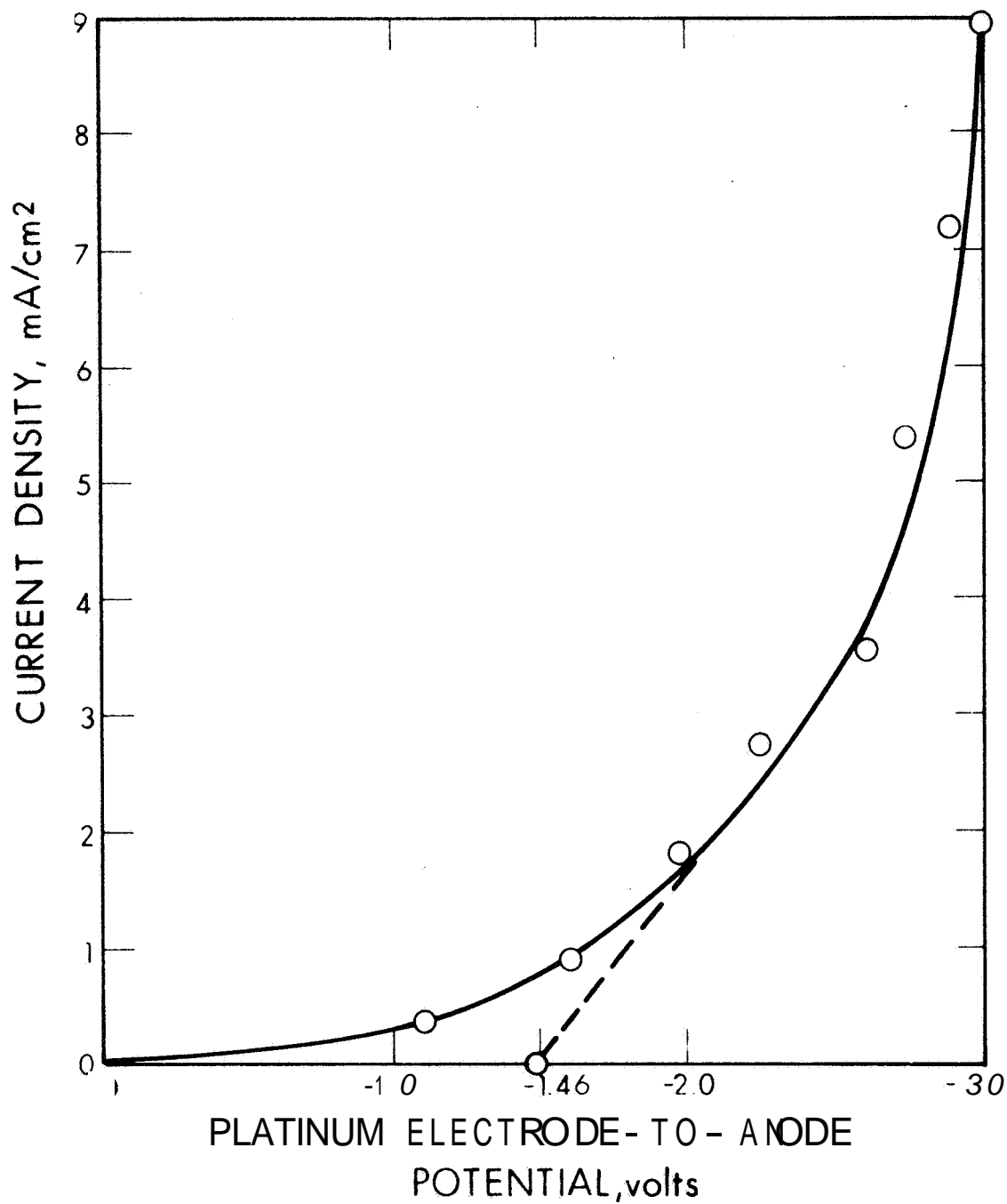
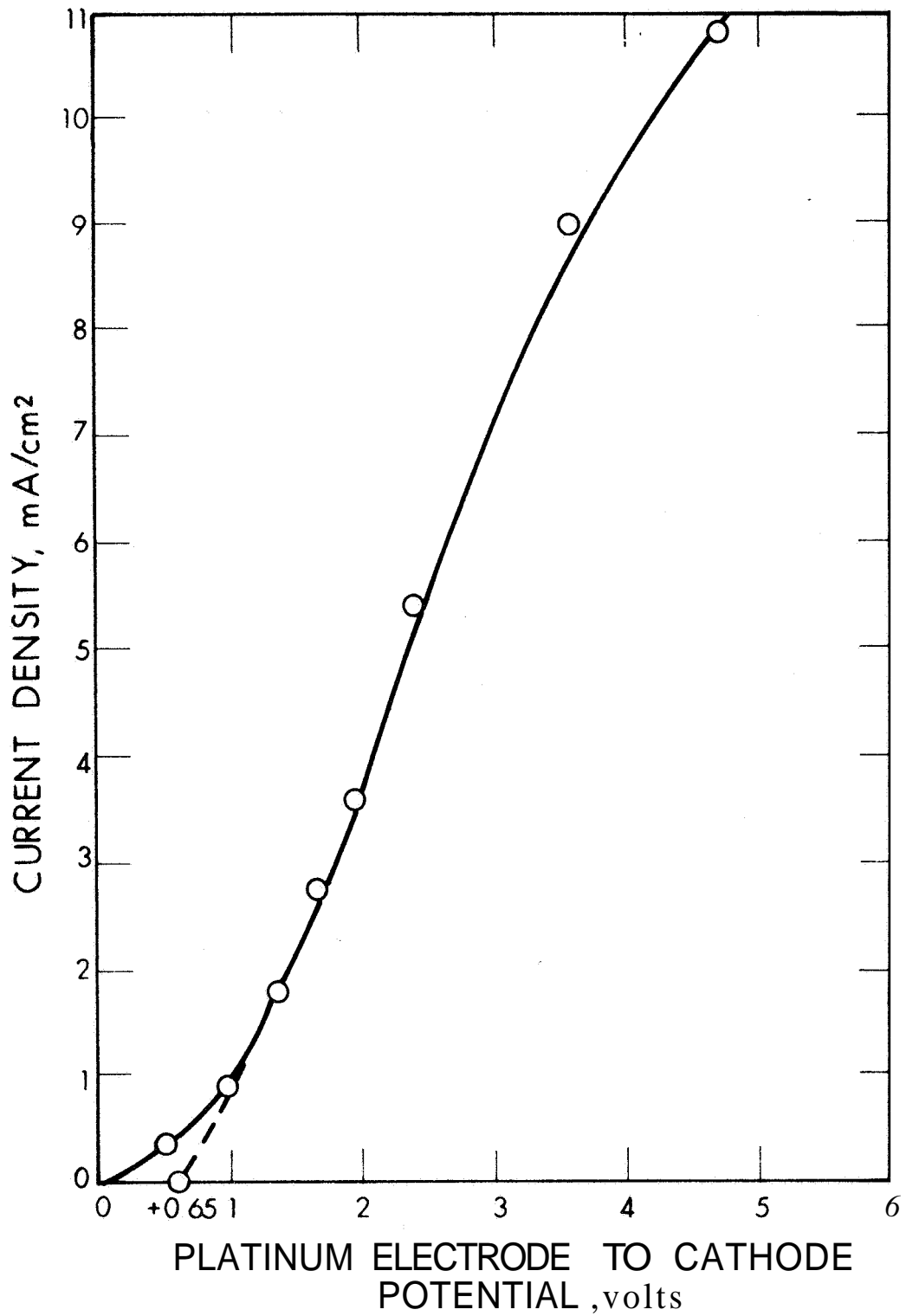Figure *4*.   Anode Polarization Curve
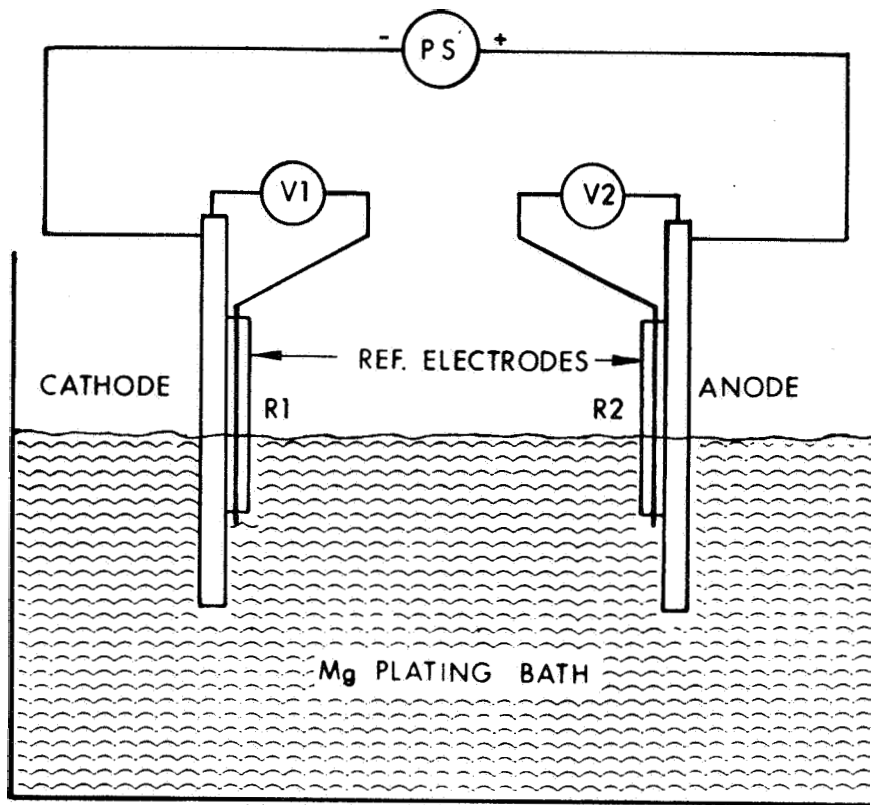
Figure 5.   Cathode Polarization Curve

Figure 6. Decomposition Potential Measurement Cell Schematic

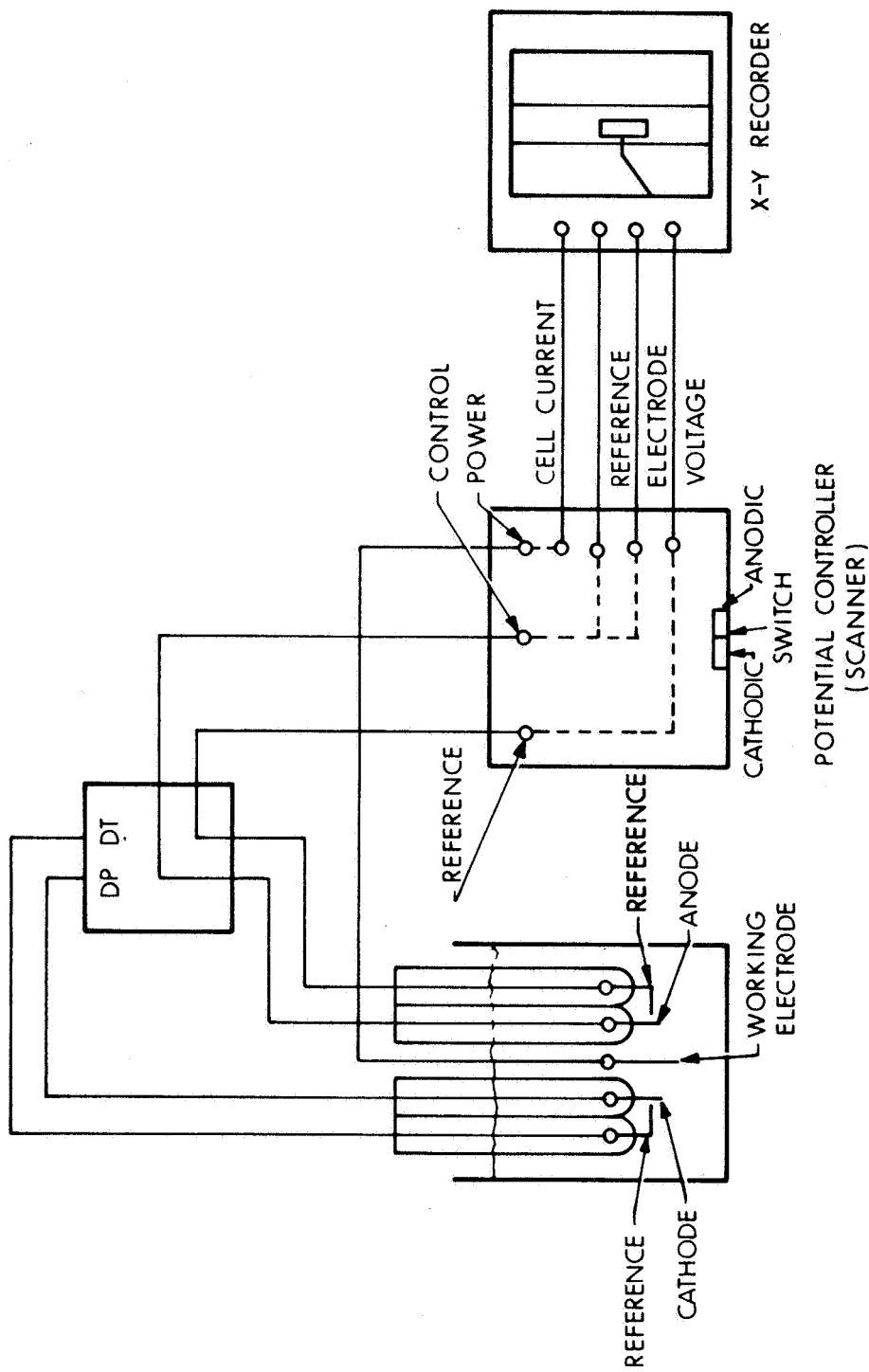Figure 7. Schematic of Apparatus for Polarization Curve Study

33

73624188

solutions should be conductive.   Thus, the sequence for screening candidate solutes in an ethereal solution for codeposition is:

    a.   Determine the solubility of the salt in ether and aluminum plating solution.

    b.   Evaluate the conductivity of suitable solute-ether system.

    c.   Measure the polarization curves of solute-ether systems that show reasonable conductivity.

Solubility and conductivity: The several metals which are possibilities for codeposition with aluminum are titanium, magnesium, copper, beryllium, manganese, and zinc.   Solubility and conductivity tests were performed on anhydrous salts of these metals in diethyl ether and in the aluminum plating solution. The results of testing with the 35 salts are shown in Table VII. The degree of solubility of each salt is categorized as: **(1)** insoluble (less than 0.1 gram in $5 \times 10^{-5} m^3$ (50 ml) of solvent), (2) slightly soluble (less than 1 gram in $5 \times 10^{-5} m^3$ of solvent), and *(3)* soluble (greater than 1 gram in $5 \times 10^{-5} m^3$ of solvent, with actual value listed).   All the salts tested were either insoluble or slightly soluble in diethyl ether.   Some of the halides were more soluble in the aluminum plating solution (especially the chlorides).   The increase in conductivity is not only a better gage in evaluating the degree of solubility, but also in ascertaining how much the salt ionizes in the solvent.   For example, titanium acetylacetonate was insoluble when measured physically, but the conductivity of the ethereal solution increased by 10^7.   This indicates that only very **low** concentrations of ions are required to yield a great magnitude of change in conductivity.   The addition of salts to the aluminum plating solution did not alter its conductivity.

34

TABLE VII

TEST SUMMARY SOLVENT SYSTEMS

Solute	Diethyl Ether*		AlCl$_3$-LiAlH$_4$ Plating Solution**	
	Solubility	Conductivity ohm^{-1} cm^{-1}	Solubility	Conductivity ohm^{-1} cm^{-1}
1. Titanium acetylacetonate	Insoluble	2.3×10^{-6}	Insoluble	8.9×10^{-5}
2. Titanocene dichloride	Insoluble	1.78×10^{-6}	Insoluble	2.2×10^{-4}
3. Titanium tetrabromide	Slightly soluble	3.8×10^{-5}	Slightly soluble	3.4×10^{-4}
4. Titanium fluoride	Slightly soluble	1.4×10^{-5}	Slightly soluble	2.5×10^{-4}
5. Titanium boride	Insoluble	2.7×10^{-6}	Slightly soluble	1.2×10^{-4}
6. Titanic trichloride	Slightly soluble	4.9×10^{-5}	Slightly soluble	1.7×10^{-4}
7. Titanium phosphide	Insoluble	6.2×10^{-6}	Insoluble	7.4×10^{-5}
8. Manganese bromide	Slightly soluble	3.3×10^{-5}	Slightly soluble	6.8×10^{-4}
9. Manganese chloride	Slightly soluble	3.1×10^{-5}	1.5 gram/5.0 x 10^{-5} m^3(50 ml)	7.4×10^{-4}
10. Manganese trichloride	Insoluble	2.7×10^{-6}	Insoluble	9.1×10^{-5}
11. Manganese acetylacetonate	Insoluble	3.2×10^{-6}	Insoluble	7.2×10^{-5}
12. Manganese difluoride	Slightly soluble	3.7×10^{-5}	Slightly soluble	5.8×10^{-4}
13. Manganese trifluoride	Slightly soluble	4.1×10^{-5}	Slightly soluble	6.5×10^{-4}
14. Manganocene	Insoluble	5.2×10^{-6}	Insoluble	8.2×10^{-5}
15. Cupric chloride	Insoluble	4.8×10^{-6}	Slightly soluble	7.4×10^{-4}
16. Cupric fluoride	Insoluble	5.3×10^{-6}	Insoluble	9.8×10^{-5}
17. Copper acetylacetonate	Insoluble	3.7×10^{-6}	Insoluble	2.2×10^{-4}
18. Cuprous bromide	Insoluble	7.3×10^{-5}	Insoluble	1.8×10^{-4}
19. Copper ethylacetylacetate	Insoluble	5.5×10^{-6}	Insoluble	2.4×10^{-4}
20. Cuprous iodide	Insoluble	1.8×10^{-5}	Insoluble	9.6×10^{-5}

TABLE VII

TEST SUMMARY SOLVENT SYSTEMS (contd)

Solute	Diethyl Ether*		AlCl$_3$-LiAlH$_4$, Plating Solution**	
	Solubility	Conductivity ohm^{-1} cm^{-1}	Solubility	Conductivity ohm^{-1} cm^{-1}
21. Copper tetrafluoroborate	Slightly soluble	8.5×10^{-5}	Insoluble[a]	2.1×10^{-4}
22. Magnesium chloride	Slightly soluble	1.3×10^{-4}	3.4 gram/5.0 x 10^{-5} m3	2.3×10^{-4}
23. Magnesium iodide	Slightly soluble	1.7×10^{-4}	Slightly soluble[a]	1.9×10^{-4}
24. Magnocene	Insoluble	5.3×10^{-6}	Insoluble[a]	8.9×10^{-5}
25. Beryllium acetate	Insoluble	4.8×10^{-6}	Insoluble[a]	2.5×10^{-4}
26. Beryllium acetylacetonate[a]	Insoluble	8.8×10^{-6}	Insoluble[a]	1.1×10^{-4}
27. Beryllium bromide	Insoluble	4.5×10^{-5}	Slightly soluble[a]	2.0×10^{-4}
28. Beryllium chloride	Slightly soluble[a]	8.7×10^{-5}	2.1 gram/5 0 x 10^{-5} m3	1.3×10^{-4}
29. Beryllium ethylacetylacetonate	Insoluble	$7 3 \times 10^{-5}$	Slightly soluble[a]	1.7×10^{-4}
30. Beryllium fluoride	Insoluble	4.2×10^{-6}	Insoluble[a]	2.1×10^{-4}
31. Beryllium iodide	Insoluble[a]	7.3×10^{-6}	Slightly soluble[a]	8.8×10^{-5}
32. Zinc acetylacetonate	Insoluble	4.4×10^{-5}	Insoluble	2.1×10^{-4}
33. Zinc bromide	Slightly soluble[a]	6.7×10^{-5}	Slightly soluble	2.3×10^{-4}
34. Zinc fluoride	Insoluble	3.3×10^{-5}	Insoluble	1.7×10^{-4}
35. Zinc iodide	Slightly soluble[a]	5.5×10^{-5}	Slightly soluble	2.4×10^{-4}

* Conductivity of pure ether 2.7×10^{-13} ohm^{-1} cm^{-1}

** Conductivity of aluminum plating solution 1 a x 10^{-4} ohm^{-1} cm^{-1}

Polarization curve measurement: The first series of polarization curve measurements was performed on seven titanium salts in diethyl ether. When the data were plotted, all the curves were linear and extrapolated very closely to zero potential. Thus, no information on decomposition potential was learned from these measurements. The second series of measurements was performed on these same salts, but in the aluminum plating solution. The polarization curves obtained were very much those of the pure aluminum plating solution. If there were any additional plateaus, they were probably obscured when the data were plotted. The present experimental technique is really not sensitive enough for studying solutions with low conductivity or where the ratios of ionic species are of very large magnitude. Also, because of the length required for doing the voltage scan, concentration polarization probably set in and caused further difficulties.

Another technique, known as cyclic sweep voltammetry, is now useful for measuring electrochemical characteristics of solutions with low conductivity. The rapid cyclic nature of this technique bypass'es the concentration polarization and minimizes the effect of high-IR, low-conductivity solutions. The method involves subjecting the electrode under study to a repetitive triangular voltage-time sweep, usually by feeding a reference signal of this form into a potentiostat and observing the time on an oscilloscope. The schematic of a cyclic voltammetric apparatus is shown in Fig. 8. The completely assembled laboratory apparatus is shown in Fig. 9. However, the operational amplifier subassembly of the apparatus could not be made to function properly and the apparatus was modified as shown in Fig. 10. After the input square wave was converted into a triangular waveform, it was further amplified by the oscilloscope preamplifier, which also controlled the dc base level to the cell.
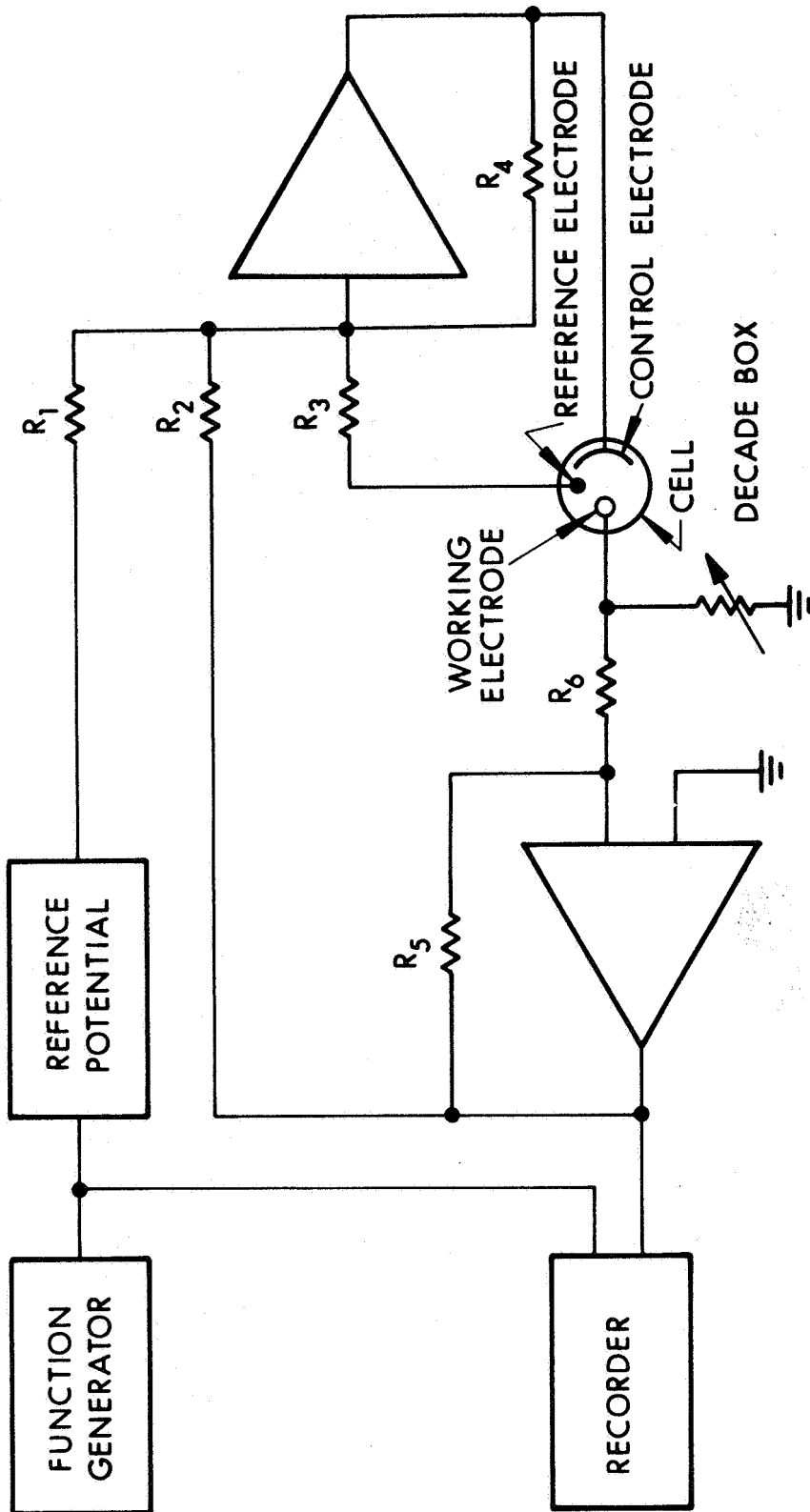
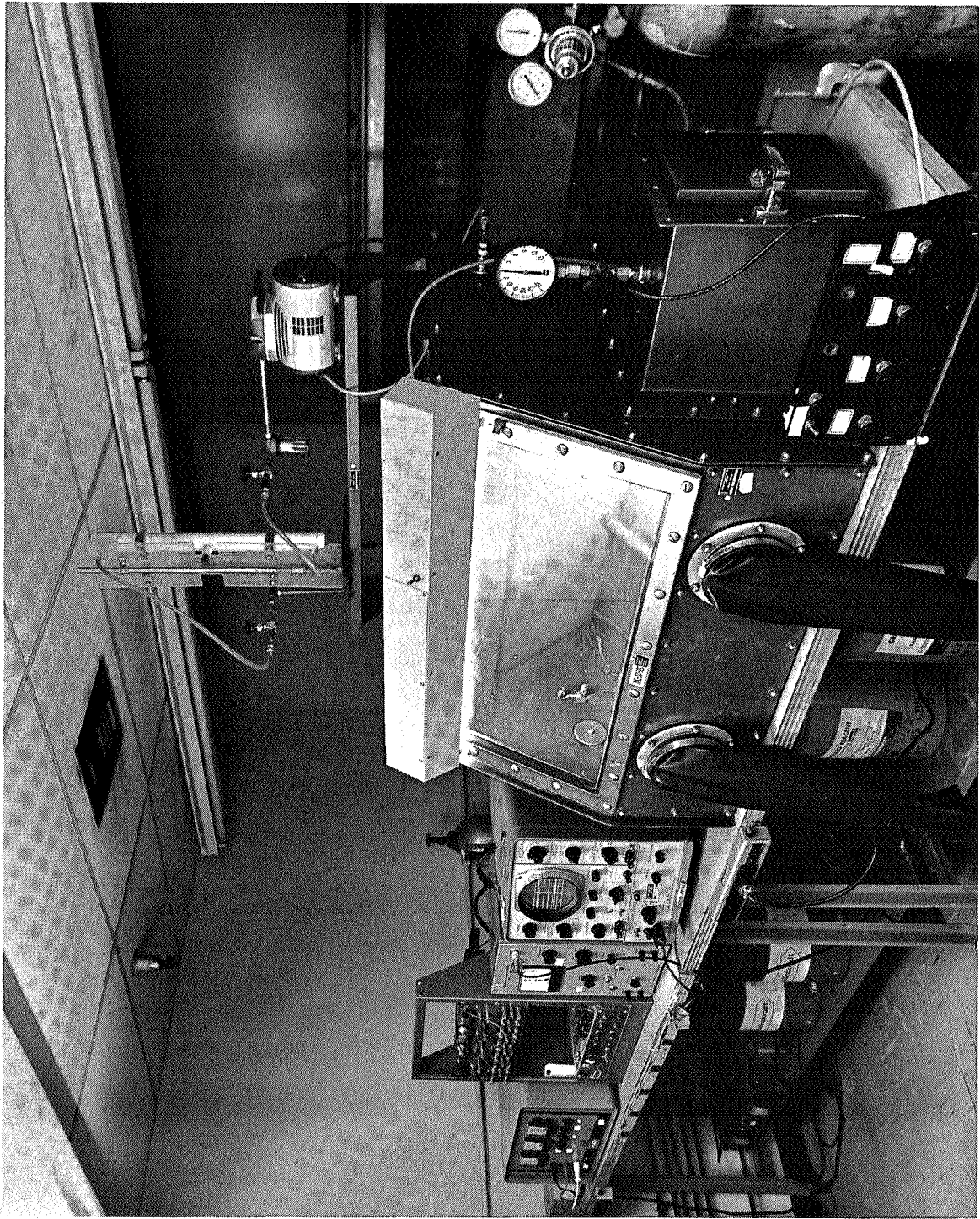Figure 8. Cyclic Voltammetry Apparatus Schematic

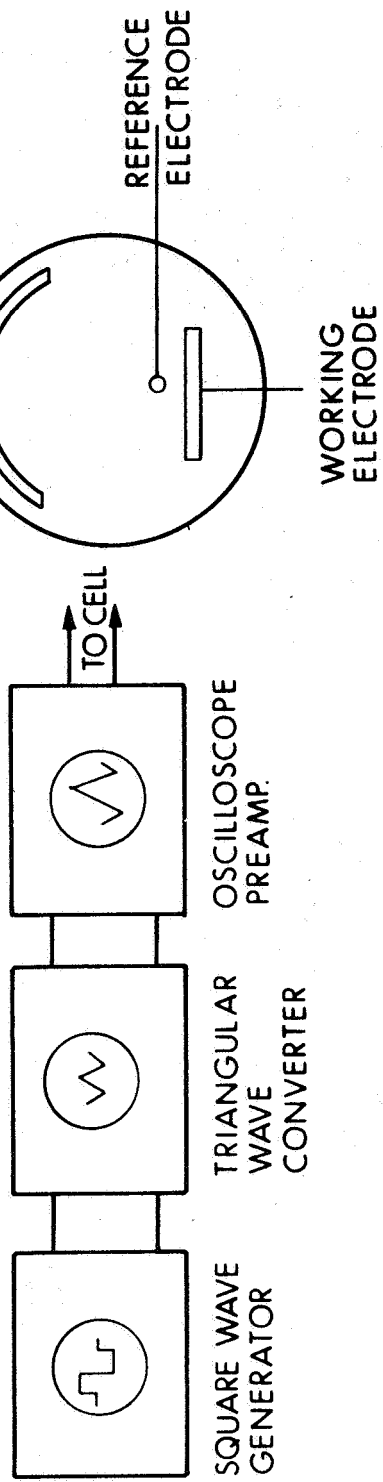Figure 9. Fully Assembled Laboratory Apparatus

Figure 10   Experimental Setup

The counter electrode (anode) was a coiled sheet of platinum gauze. The working electrode (cathode) consisted of a square plate of 0.25 mm platinum (about 1 cm^2 in area) which was spot-welded to a platinum lead. The reference electrode was a platinum wire positioned so that the tip was less than 1 mm from the working electrode. The electrodes were contained in a cylindrical glass cell with a tight-fitting TFE (tetrafluoroethylene polymer) cover with provisions for the platinum leads to the electrodes. The leads to the reference and working electrodes were enclosed within capillary tubing with TFE caps at the ends immersed in the test solution.

A solution of $AlCl_3$ (3.4M) in diethyl ether was chosen as the reference solution so that data obtained from examination (by cyclic sweep voltammetry) of other solutions of various metallic species could be used to ascertain whether such species can possibly be made to codeposit with the aluminum to form an alloy.

The dc level from the scope preamp was adjusted so that the triangular wave was always positive and only plating (and not deplating) of aluminum could occur at the working electrode.

Data for the $AlCl_3$ solution at two different frequencies and for the case of a resistor substituted for the cell are shown in Fig. 11. Analysis of the plot for the case of the resistor showed a large deviation from linearity occurring near 6V peak input (no load). As viewed on the oscilloscope, a considerable amount of rounding of the triangular waveform began to occur at this point. This indicates that the oscilloscope preamplifier is becoming current limiting and can no longer supply current in a linear manner with an increase in voltage.
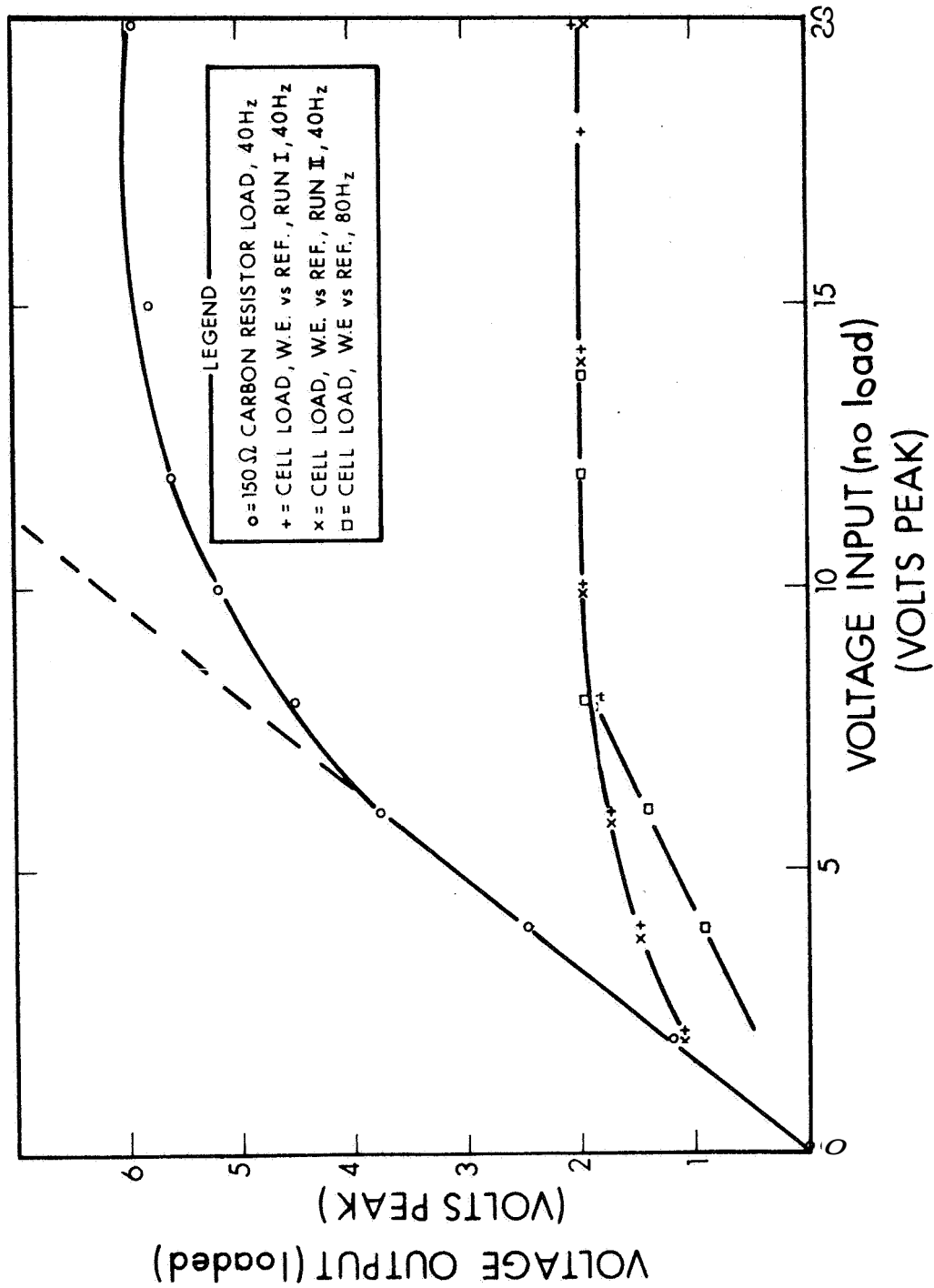
Figure 11   Output Voltage (under Load) versus Input Voltage (Load)

LEGEND

o = 150 Ω CARBON RESISTOR LOAD, 40Hz
+ = CELL LOAD, W.E. vs REF., RUN I, 40Hz
x = CELL LOAD, W.E. vs REF., RUN II, 40Hz
□ = CELL LOAD, W.E vs REF., 80Hz

VOLTAGE INPUT (no load)
(VOLTS PEAK)

VOLTAGE OUTPUT (loaded)
(VOLTS PEAK)

42

73425992

The effective impedance of the scope preamp with the 150−ohm resistor was found to be approximately 90 ohms. Since the resistance of the cell was less than 50 ohms and since current limiting was observed in the case of the 150 ohm resistor loading, the data obtained for the cell cannot be interpreted with any degree of certainty at this time. Although the validity of these data are questionable, it was noted that, although the rounding of the triangular waveform in the case of the resistive loading was very symmetric, that observed for the case of the cell was asymmetric and had a more flattened nature on the voltage increasing side of the waveform. This flattening became noticeable at 40 Hz at about 10V peak input (no load) to the cell or at a cathode voltage of 2V (relative to the platinum reference electrode). A typical output waveform is shown in Fig. 12 for the case of no−load input voltage of $15V_P$ *(40* Hz).

Part of the rounding observed is undoubtedly caused by the resistive component of the cell but the flatter portion of the curve may result from the electrochemical reaction taking place (i.e., the plating of aluminum). Before more meaningful data can be obtained from the cyclic sweep voltammetric study, the present experimental setup must be replaced with one that has the desired power capabilities (at the desired frequencies) without distortion or rounding of the triangular wave taking place. Ideally then, one would like to modulate a power supply feeding the cell. Consultation with the manufacturer of the potential controller revealed that this unit would have the power capacity desired, and an auxiliary power is available for boosting the maximum output if this should be necessary at a later date. Testing of the unit revealed that it could be modulated and was not frequency limited at frequencies as high as 1 kHz, which is probably higher than would be required for the cyclic sweep study. This unit will be modified to the required specifications for future work.
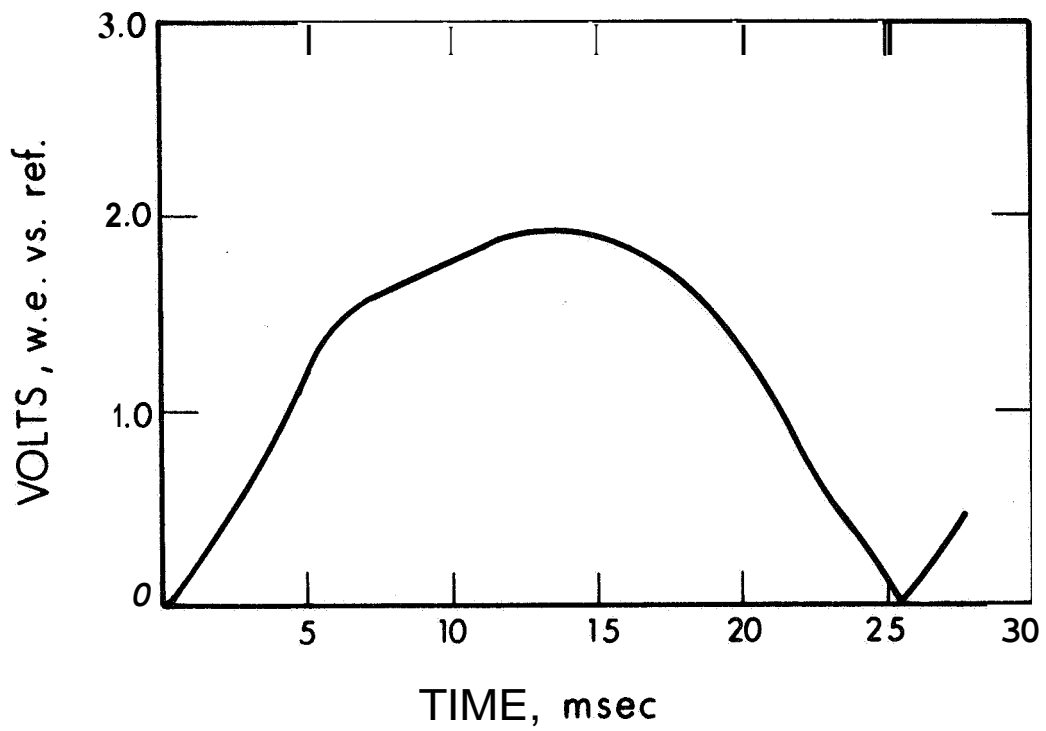
Figure 12. Output Waveform (15 V_p Triangular Waveform Input, *40* Hz)

Process Development

The primary mission of the process development phase is to integrate the essential parameters singly sought out in the electrotechnology studies into a practical laboratory process. Data generated by the laboratory operation are to serve two purposes: to feed back information to further refine the process, and to lay bases for converting the process to a pilot plant operation.

Magnesium plating process. - Experimental results under the electrotechnology study indicate that the magnesium plating process requires a more complex technique to achieve a practical, thick magnesiumdeposit. Some of the essential features incorporated include continuous bath agitation, continuous bath filtration, continuous bath concentration replenishment, and continuous addition of alkyl halide.

A laboratory plating assembly designed to meet all the above requirements was constructed. The completed assembly is shown in Fig. 13 and the schematic of the assembly is shown in Fig. 14.

The entire assembly is a closed, air-tight system made of glass. The plating tank is a large glass dessicator with a fluoro-rubber seal between the lid and the jar. There is a conforming anode in the bottom of the jar; suspended and centered above is a stainless steel convex master. The master is suspended by a shaft which passes through a seal to a rotation motor on the outside.

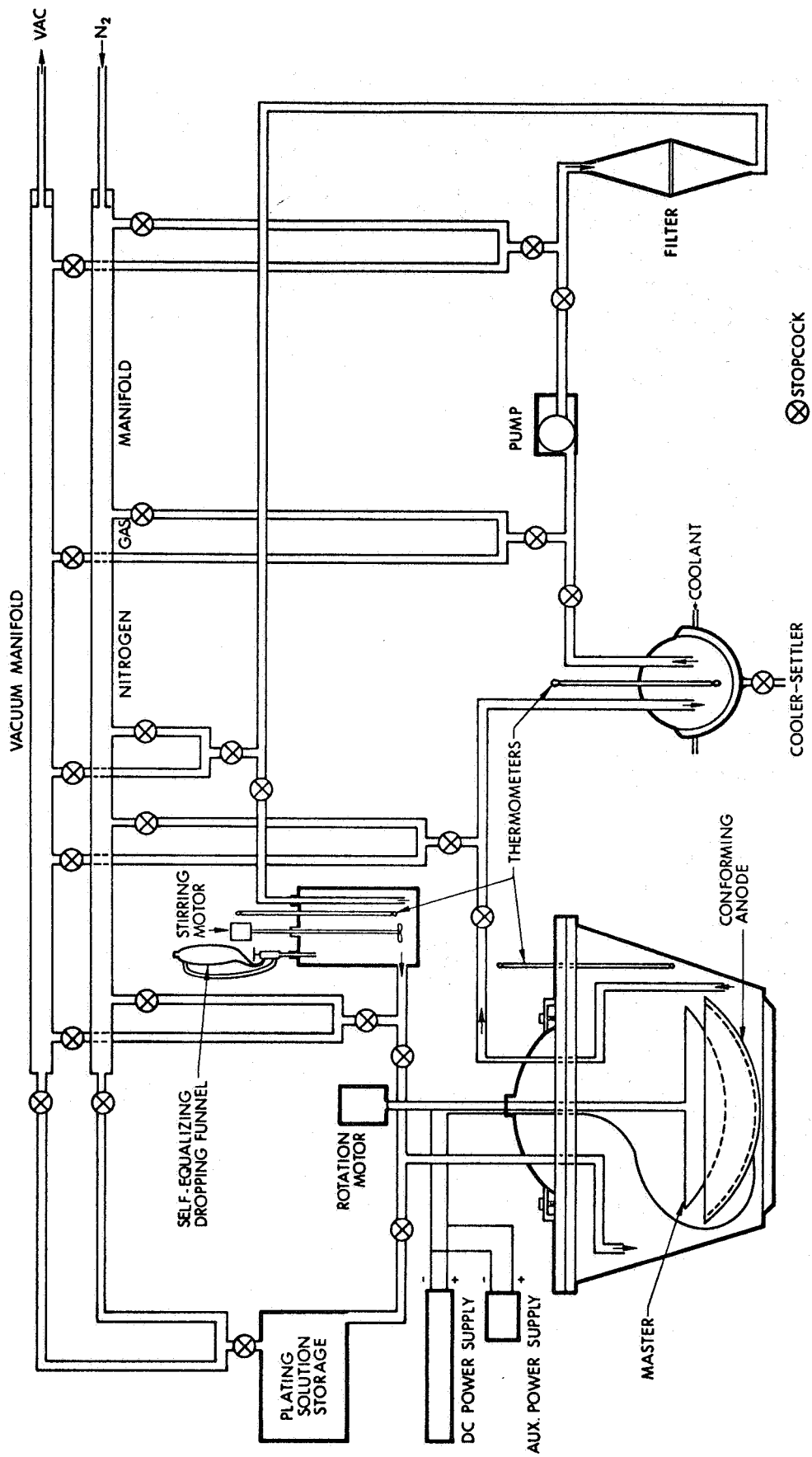Figure 13. Laboratory Magnesium Mirror Electroforming Assembly

46

Figure 14. Schematic of the Magnesium Mirror Electroforming Apparatus

47

73623223

A pump is employed in the line for circulation. The solution reaches a small flask with a cooling water jacket, where the particles settle to the bottom. It is then pumped through a coarse fritted-glass filter into a jar where the alkyl halide and fresh plating solutions are added. From this jar, the solution drains back into the plating bath. The solution is held in the storage tank while the mirror is removed or set back up or when part of the line is being replaced.

Five TFE stopcocks are used in the line so that any one part can be fixed, changed, or purged while keeping the rest sealed. In each section there is a tee with a TFE stopcock. Each of these stopcocks leads to one of two manifolds (one for vacuum and the other for nitrogen gas).

Thermometers are placed in various locations in the system so that the temperature in each area can be monitored.

A dc power supply is the main power for plating. An auxiliary battery power supply is hooked onto the main dc power supply in case of power failure.

All the stopcocks which come in contact with the solution are made of TFE. In like manner all glass joints have TFE liners. The master is supported and rotated with a steel rod which operates through a TFE rotating gland with a rubber O-ring.

During a shakedown run conducted on the completed magnesium electroforming assembly, several glass joints were cracked because of internal stresses. These stresses existed because of improper annealing of the glass parts during fabrication. The broken portions were repaired and care was exercised in annealing them

properly. Another shakedown was conducted and no further cracks developed. A manometer has been connected to the assembly to sense internal pressure. It was noted that the internal pressure was approximately at 4×10^{-2} m Hg during operation. An overhanging exhaust hood has been installed over the entire assembly to draw out any organic fumes in case of a leak.

An electroforming run was conducted during this period. After four hours of operation, the pump (prime mover of the system) began to choke. The run was terminated at that point and the pump disas— sembled for examination. It was noted that the liner of the pump had swelled about 25%. The iiner is fabricated of an elastomer material. Previous compatibility tests for a similar plastic material have shown that the material is resistant to ethereal solutions. It could be that the chemical resistance of the elastomer is very much different from the plastic. Another explanation for the failure is that the elastomer may be suitable for static use in ethereal solution but not suitable for dynamic uses. The pump was refitted by the manu-facturer with a polyvinyl alcohol liner which has much higher resist-ance to ethereal solutions. No further variable experiments were conducted with the test assembly because the electrochemical study phase of magnesium plating was not finalized.

Hardened aluminum plating process. – In the studies on optimizing the hardened aluminum plating bath, the process in many ways is very similar to conventional plating processes. The primary difference is that the process must be carried out in an inert atmosphere. The final process design may be best discussed through some of the problems encountered and how the plating equipment was modified to rectify those problems.

In the course of electroforming the 10.2 x 15.2 cm flat plates it was observed that the loss of bath solvent was substantial and had to be replenished quite frequently. The loss was the combined effect of evaporation due to heating and the operation of the vacuum-pressure filtering system. The plating apparatus was then modified accordingly to minimize the loss of bath solvent. The two changes were: (1) the fabrication of a stainless steel lid which also acts as a reflux condenser to replace the polyvinyl-chloride plastic lid, and (2) installation of a continuously circulating filter system replacing the vacuum-pressure mode of filtration.

The cover is made of 1.6 mm 302 stainless steel. The cover is hollow with a flat top and the bottom shaped like an inverted pyramid. Wells are provided for insertion of electrodes and circulation pumping through the cover. These wells have TFE inserts to insulate the electrodes and metal tubing from the body of the cover. One 6.35 mm tube fitting is welded at each end to fasten coolant inlet and outlet lines. The design of the cover-reflux condenser is shown in Fig. 15.

The incorporation of these two changes not only minimizes the loss of bath solvent, but reduces the need for an operator to watch the plating bath constantly to maintain the plating solution level and to eliminate other condensates inside the glove box, which in time will extend the life of the gloves, gasket, etc. The continuously circulating filter system is more effective in removing anode slime and other insoluble particles because the rapid circulatory motion provides a much better mode of agitation.
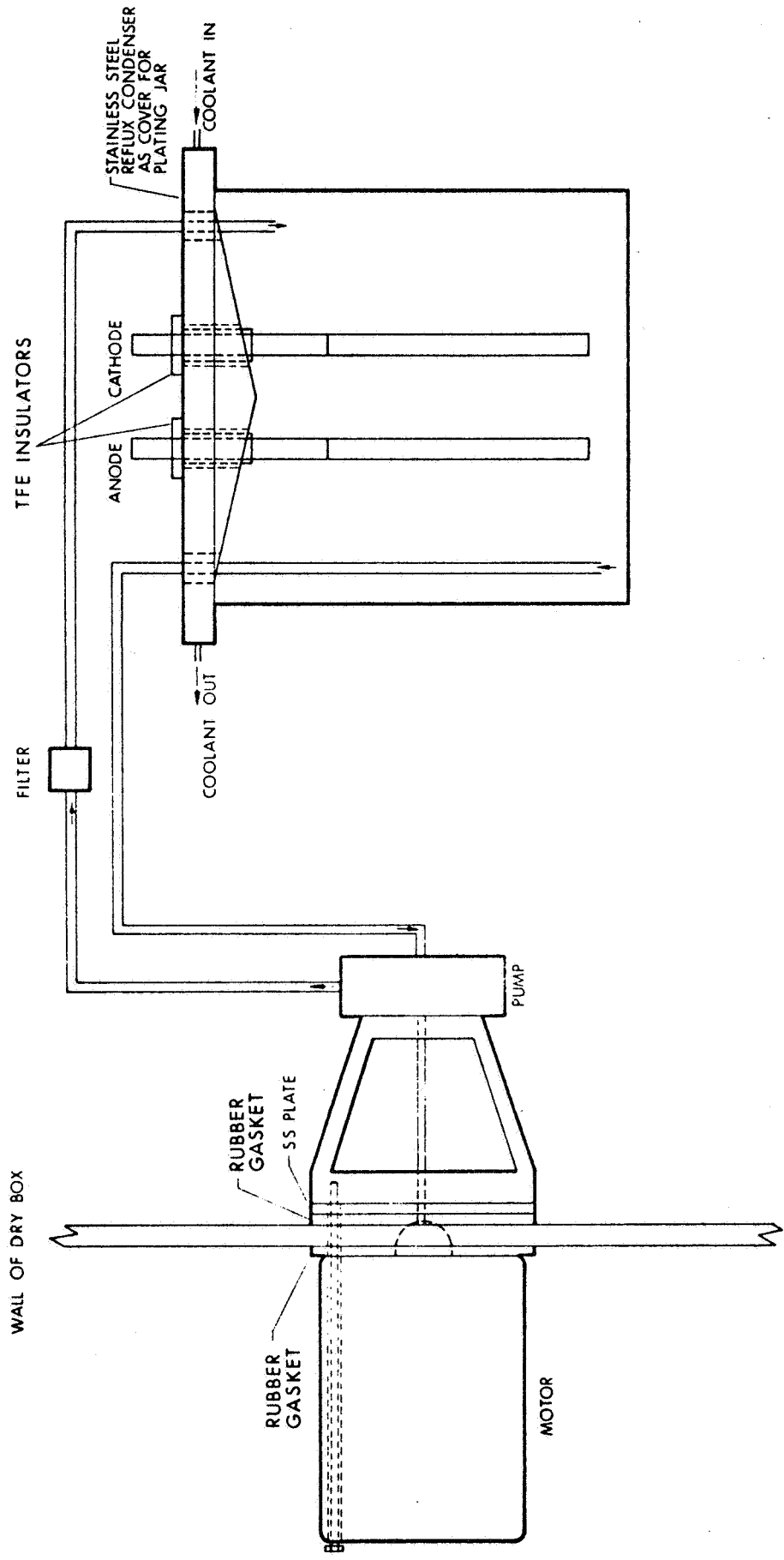
Figure 15. Plating Cell Cover - Reflux Condenser Pump-Filter

51

<u>30.5-cm mirror electroforming cell</u>.

Safety engineering; The 30.5-cm mirror plating cell has been moved and the electroforming operation is being conducted in a special facility. The 30.5-cm mirror electroforming cell contains 0.0567 m^3 of ethereal electrolyte representing a potentially high safety hazard to personnel and surrounding structures.

The cell is now located in an isolated area as shown in Fig. 16. The completed safety features include the following:

a. The entire cell is surrounded with a protective, fire-controlled bunker with foot-thick filled walls.

b. The bunker is designed to release the expanding gases with minimum hazard to personnel and adjacent facilities.

c. Safety systems are designed with redundancies to reduce human error.

d. Heat, pressure, and ether vapor sensors are included to detect abnormal operation and provide a warning of danger.

e. Emergency electrolyte dump and chemical deluge systems are provided.

f. A room venting system with a minimum venting velocity of 7.070 m^3/min is provided.

Cell assembly: A cell for electroforming the 30.5-cm mirror was constructed based on findings of the hardened aluminum plating process.

The essential components are:

• The rotating fixture (Fig. 17) and its attachment to the glove box.

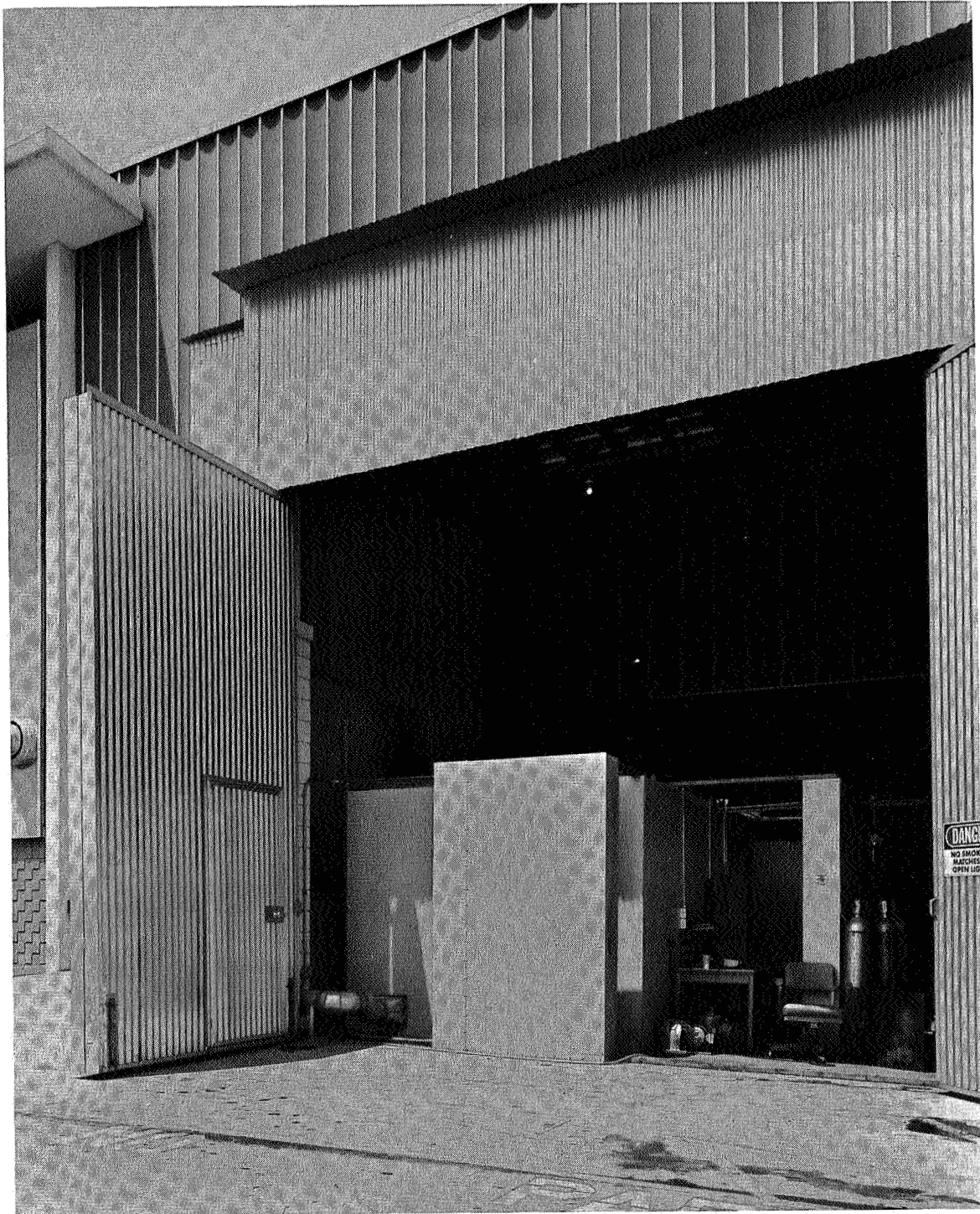o The nickel mirror master for the 30.5-cm mirror electroform (Fig. 18).

Figure 16.   Electroforming Facility

BEARING

4 BOLTS THROUGH
BOTH PIECES AND
TOP OF BOX
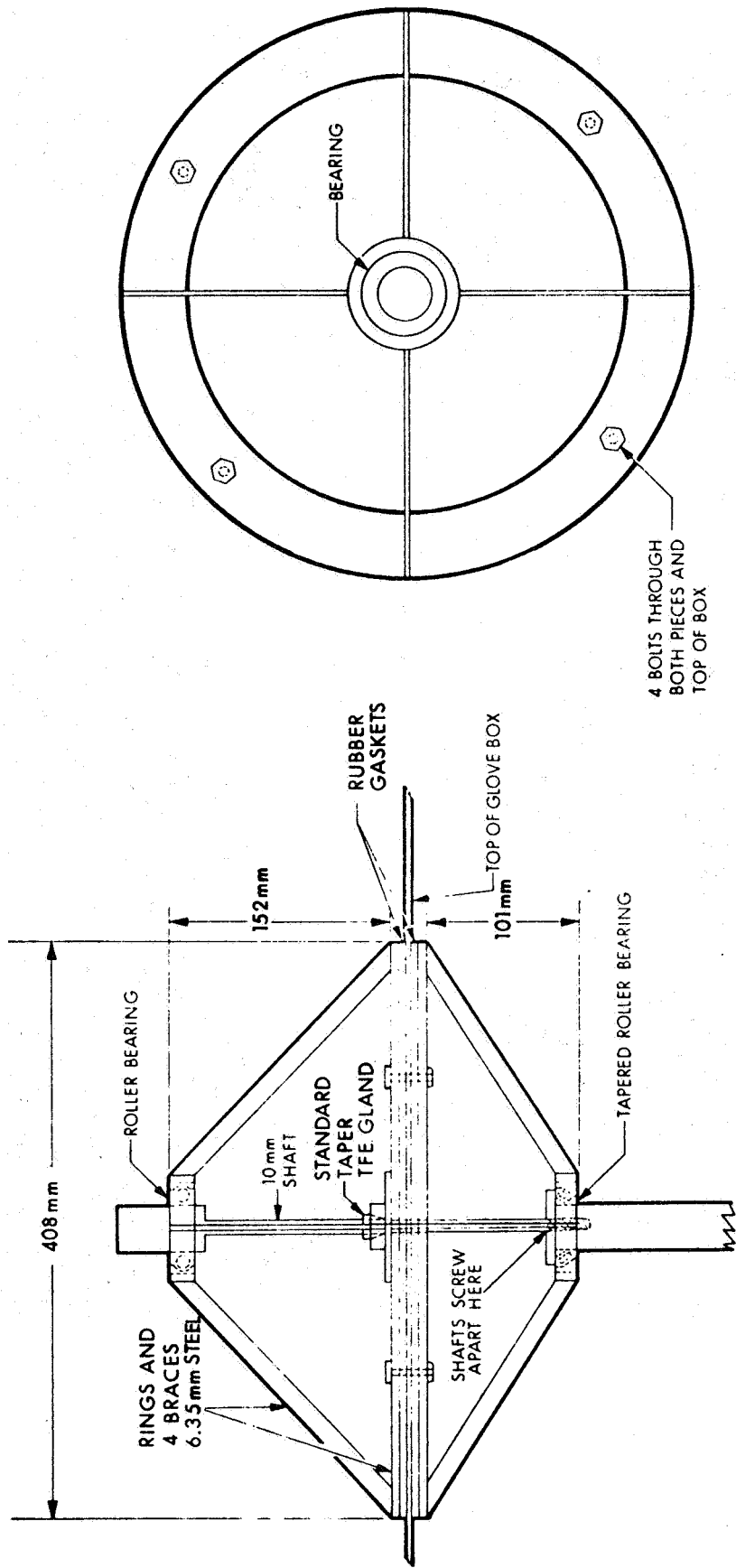
PLAN VIEW OF THE CIRCULAR BRACE

RUBBER
GASKETS

TOP OF GLOVE BOX

152mm

101mm

ROLLER BEARING

10mm
SHAFT

STANDARD
TAPER
TFE GLAND

TAPERED ROLLER BEARING

408mm

RINGS AND
4 BRACES
6.35mm STEEL

SHAFTS SCREW
APART HERE

ELEVATION VIEW OF COMPLETE ROTATING MOUNT

Figure 17.   Rotating Fixture, 30.5 cm Mirror
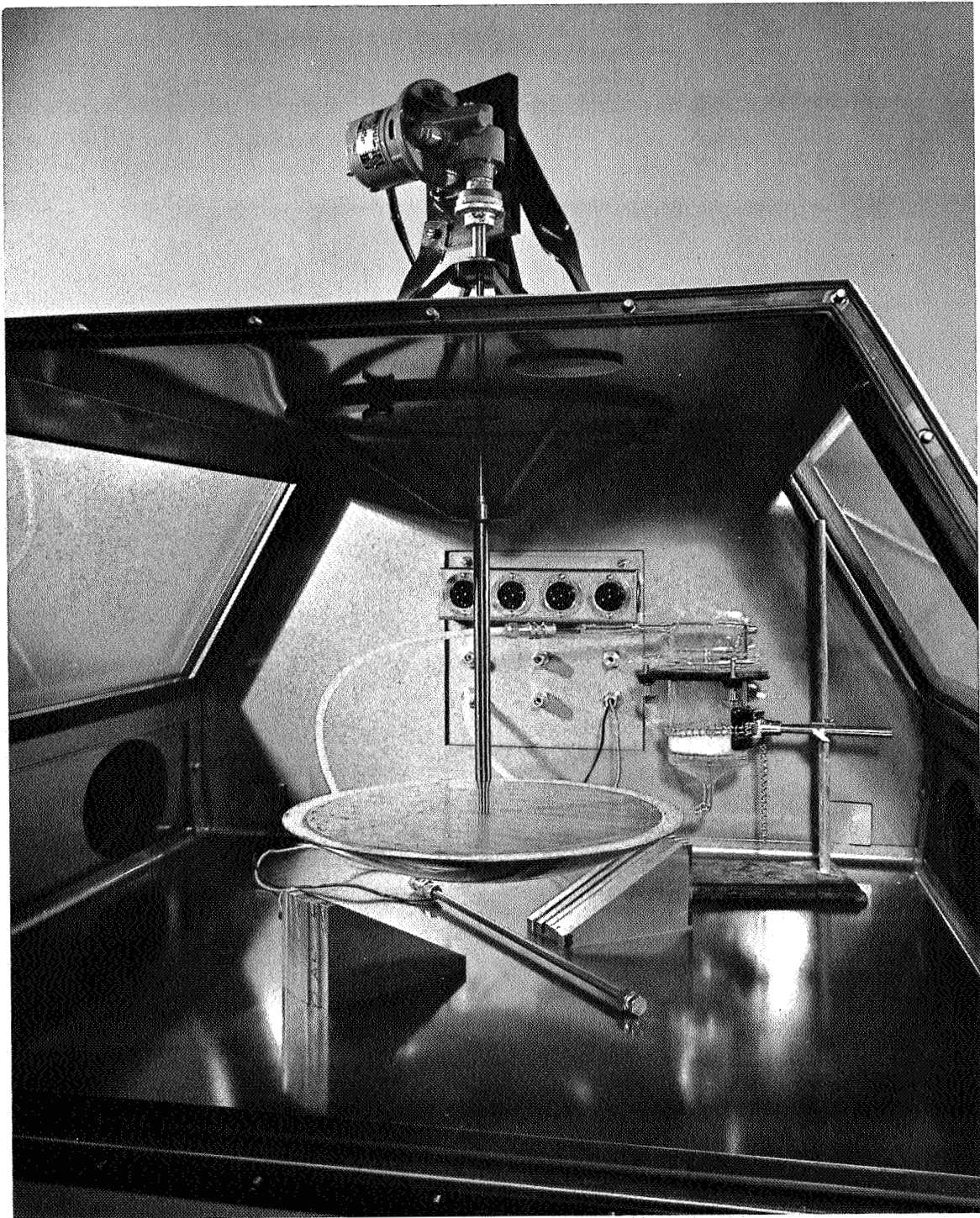
7362371 6

Figure 18. **30.5-cm** Mirror Electroforming Cell with Tank Removed
to Show Nickel Master

55

- Filtration and continuous circulation system.

- Plating tank

  The steel tank is coated with a phenolic finish to prevent corrosion by the plating solution.

- Conformal anode pack

  The pack consists of four to eight wedges tapered to the curvature of the mirror master. The wedges, spaced equally and held together with a special ring, are shrouded in TFE cloth; all the remaining metallic surfaces are coated with epoxy. The design of the anode serves two purposes:

  (1) To determine the throwing power of the anode by the variation in number and spacing of the wedges.

  (2) To eliminate the restriction of electrolyte circulation in the case where a full conforming anode is used.

  The anode pack and the nickel mirror master are shown in Fig. 19.

- Gusher lines

  The gusher lines are perforated polyethylene tubes placed under the mirror master. The filtered solution is returned to the bath through these tubes in fine divided streams.

- Reflux condenser cover

  The cover minimizes the loss of bath solvent through evaporation by serving as a cooling surface for the plating cell.

- Cooling system

  The cooling system is composed of a compressor and a heat exchanger. The temperature of the bath solution is maintained by circulation through the heat exchanger.

The polyvinyl alcohol liner in the circulation pump has shown no deleterious effects for 40 hours of continuous pumping of the ethereal plating solution,
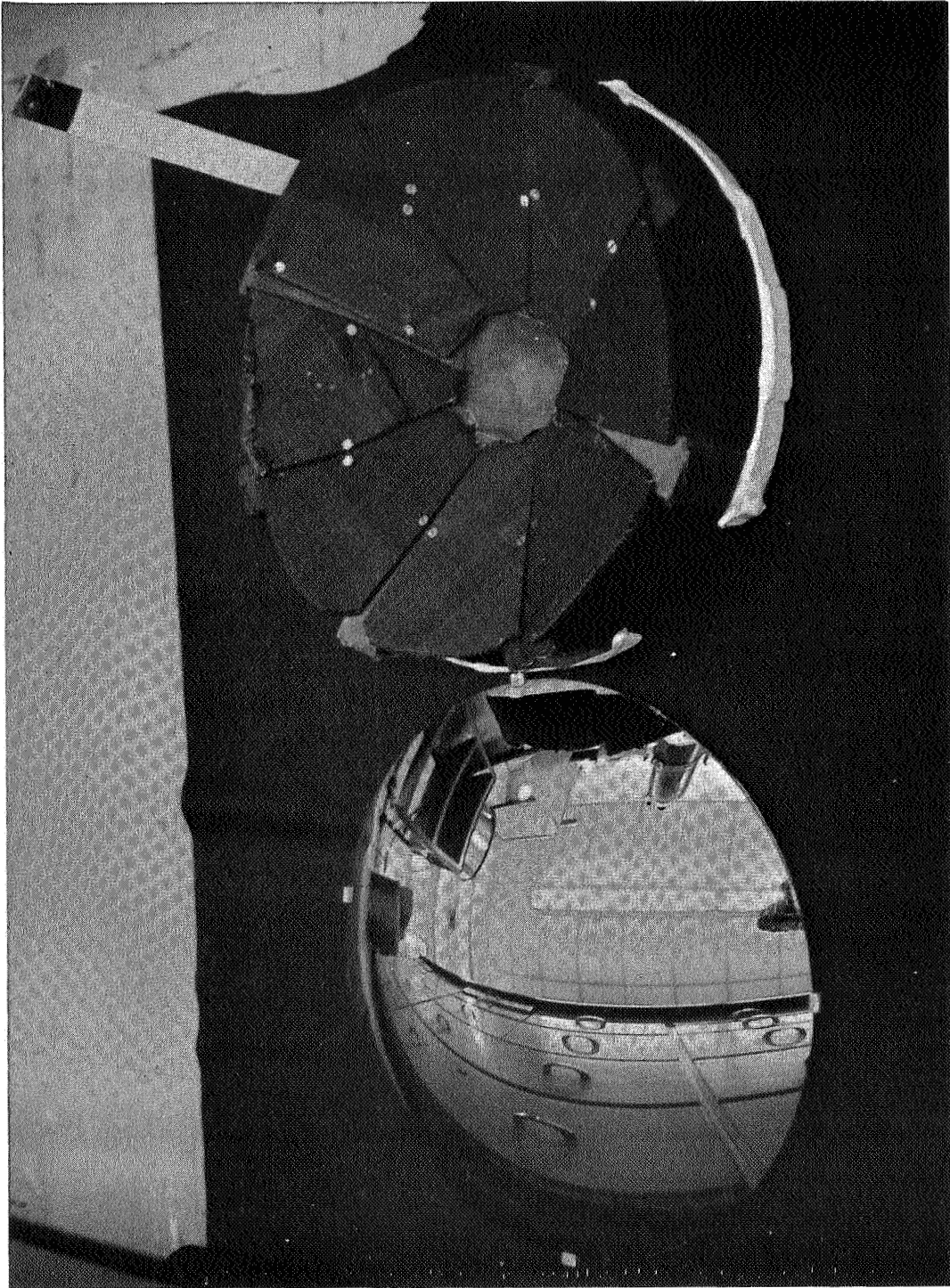
Figure 19. Anode Pack and Nickel Mirror Master

The schematic for the entire cell is shown in Fig. 20. The plating section of the electroforming cell is shown in Fig. 21, and the entire electroforming cell is shown in Fig. 22.

Electroforming Studies

To properly accredit the practicability of plating baths, it must be demonstrated that: (1) an electrodeposit can be built up to a sufficient thickness (> 0.38 mm), and (2) the deposit possesses desirable mechanical and chemical properties.

Magnesium bath. - When a thickness of greater than 0.12 mm of electrodeposit is attempted from the magnesium,plating bath, dendrites and sponge begin to form. Soon, all the available current goes to the formation of dendrites and loose sponges; thus, the current efficiency for coherent deposit approaches zero. Our work has indicated that to build up a deposit greater than 0.12 mm from the magnesium plating solution, an alkyl halide must be added continuously in an appropriate quantity to dissolve and retard the formation of dendrites and sponges. However, this technique of addition is quite critical and has not been refined to the point where flat plates of 0.38 mm thickness can be electroformed successfully.

There are factors which affect the nature of the deposit. Considerations must be made to define the electrode reaction products. This area of study is more important for the successful electrodeposition of magnesium than for aluminum because the reaction products at the anode in the case of the former are not soluble metallic species but gases and organic compounds resulting from the electrolytic dissolution of the organic electrolyte. Therefore, not only
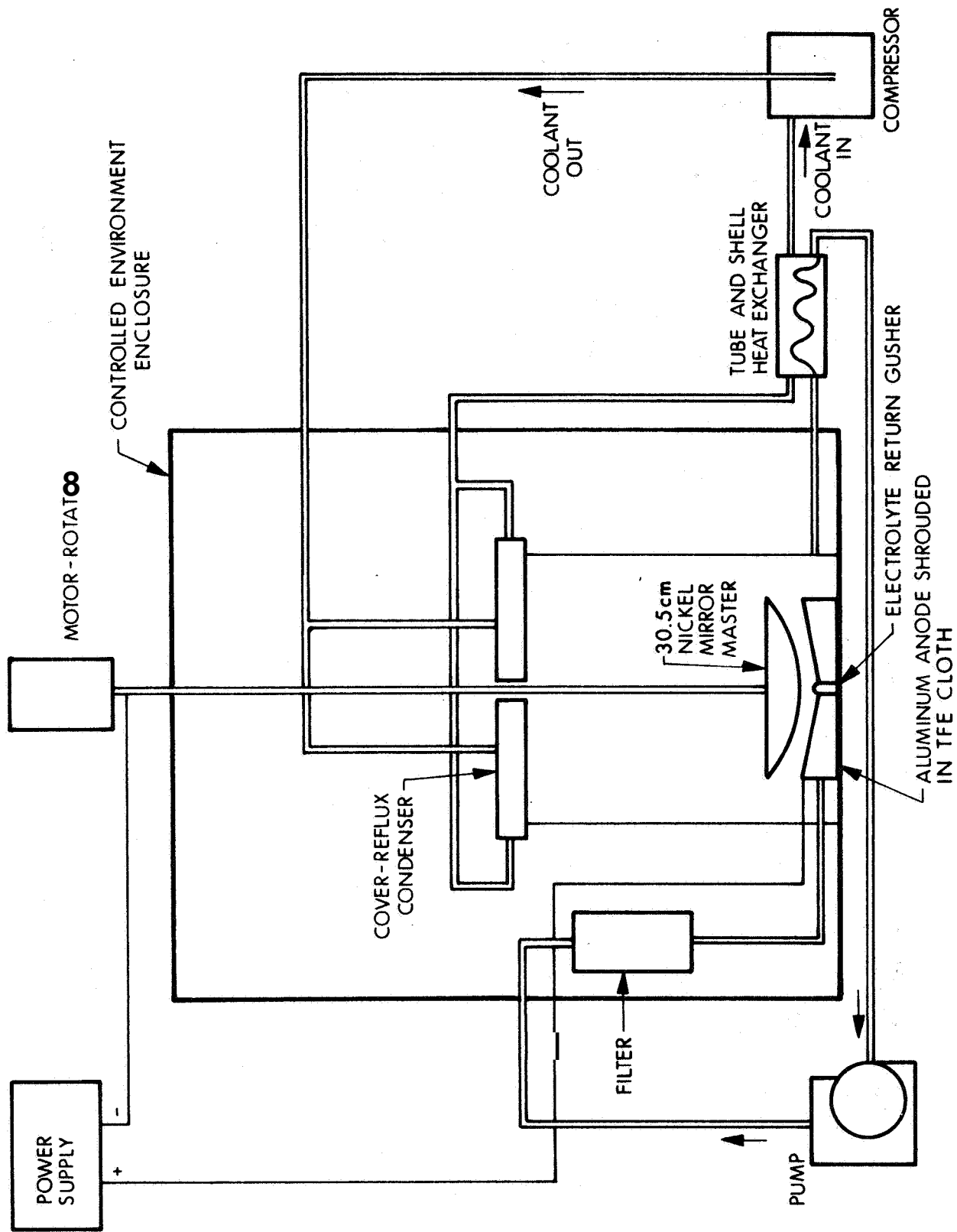
58
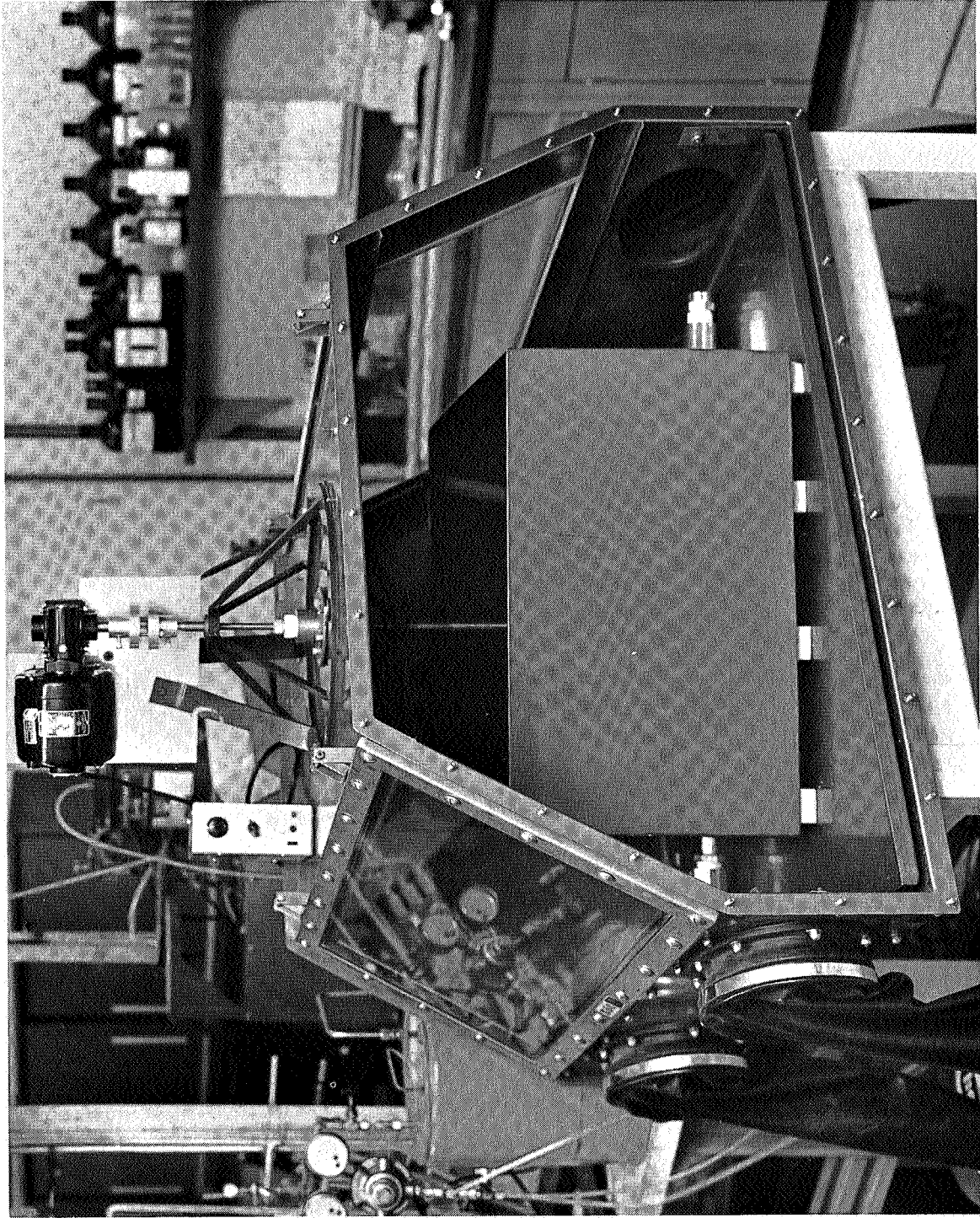
Figure 20. Schematic of 30.5-cm Mirror Electroforming Cell

Figure 21. Electroforming Cell, Plating Section
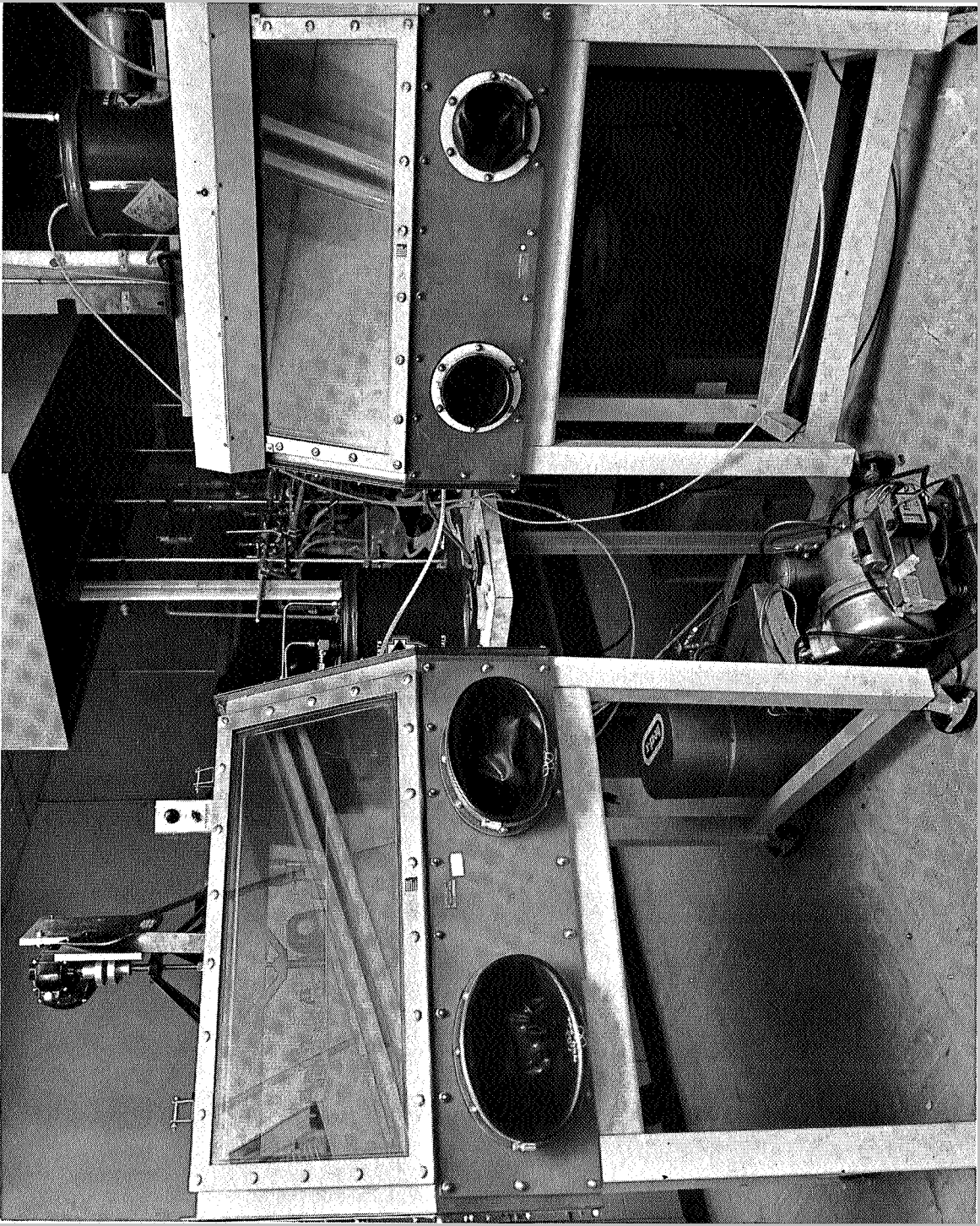
GO

Figure 22   Electroforming Cell Assembly

must the magnesium in the plating bath be replenished externally, but the anodic by-products, which have a deleterious effect on the deposit, must be rendered chemically and electrochemically inactive.

Once the basic reactions have been ascertained, a baseline can be formed to surmise the effects of the reaction products upon the electrodeposited metal and thus indicate the course to take to counteract any adverse effects. One such adverse effect is the autodecomposition of the magnesium plating solution. The practicability of the magnesium plating process cannot be realized until this instability is eliminated. Also, since the magnesium bath has a relatively low concentration of electrolytes, the solution must be stirred vigorously to minimize concentration polarization. Some agitation is effected by the circulation of the bath solution but the larger portion of the agitation is provided by bubbling dry nitrogen gas through the bath solution.

Although there are no apparent changes in the grain structure of the deposit in the temperature range $293^{O}K$ to $318^{O}K$, the chemical side reactions which accompany the electrode processes become more prominent at the higher temperatures. To minimize autodecomposition of the electrolyte, the bath temperature must be kept below $298^{O}K$. At $313^{O}K$ the autodecomposition is accelerated to such a rate that it renders the bath solution useless within 3 to 4 hours. Once the above problem areas have been studied more extensively, the bath solution can be optimized.

Aluminum and aluminum-magnesium baths. - It was noted that the
operation of the pressure-vacuum filter system was not adequate in
filtering the solution, nor in providing enough agitation. Also,
bath solvent that evaporated and condensed in the glove box greatly
accelerated the deterioration of gaskets and gloves. The large.
flat-plate electroforming was halted after three runs, and the plating
apparatus was modified. Electroforming of large flat plates was
resumed when the modification on the plating apparatus was completed.
It was found that both the continuous filtration system and the
cover-reflux condenser performed well within their designed speci-
fications. As a result, there was definite improvement in the
appearance of the electrodeposit, in addition to a drastic reduction
in solvent loss. Two 10.2 x 15.2 cm flat plates were electroformed
from both the magnesium-aluminum bath and the mixed-ether (high
boiling) bath. The front and back of one of the flat plates electro-
formed from the mixed ether is shown in Fig. 23. Notice the modular
cluster at the edges instead of long trees. The grains are exceed-
ingly fine, thus giving a very smooth overall appearance. The
thickness of the plate shown is 0.96 mm.

The magnesium-aluminum bath is a mixture of the aluminum bath
and the magnesium bath solutions. Our previous work in the attempt
at codeposition with this bath resulted in a plating that appeared
to be considerably stronger than that from the Brenner aluminum
bath. This was verified by tensile tests. Spectrograph analysis
of the resultant plates indicated that codeposition of aluminum-
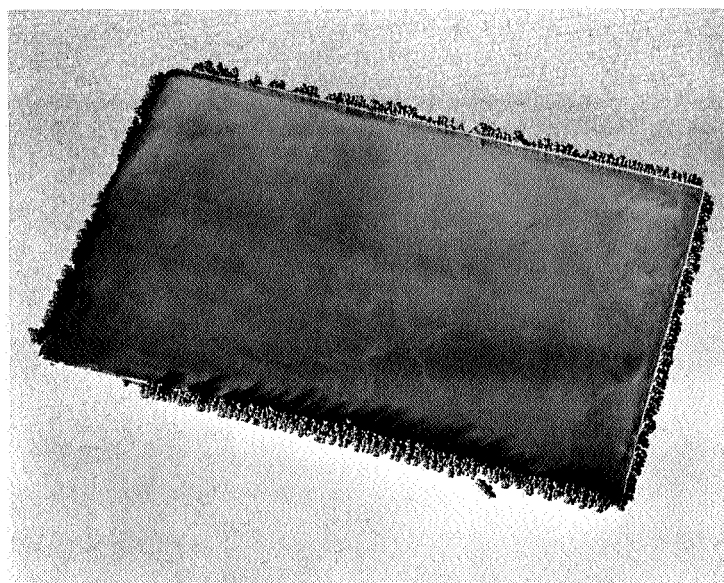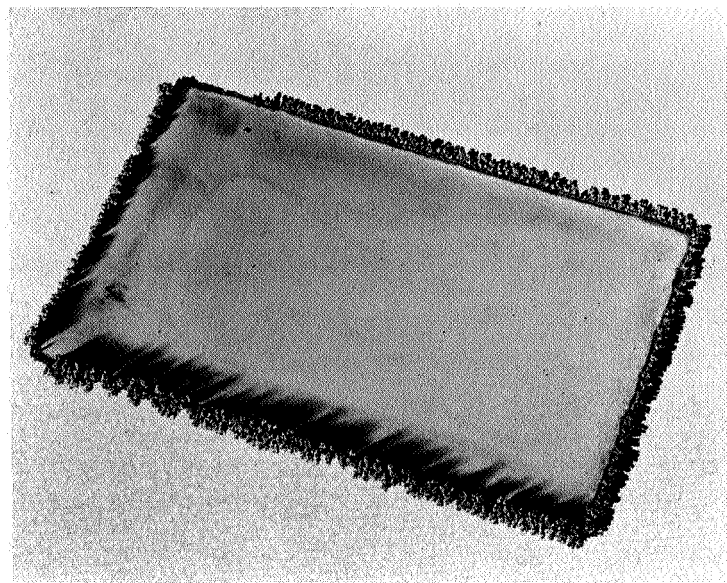magnesium did not occur.

Figure 23.   10.2 x 15.2-cm Plat Plate Electroformed
in Mixed Ether Bath

64

The mechanism of hardening without codeposition has not been investigated in depth. It has been surmised that the hardening could be due to some change in the electrochemical polarization characteristics of the bath during deposition. It was uncertain whether this polarization change is due to either the addition of the magnesium compound component or the mix solvent component of the magnesium plating solution. In furthering the investigation to determine which additive is responsible for the hardening, flat plates were electroformed in baths with the addition of only one or the other component of the magnesium plating solution to the aluminum bath. Performance of physical tests on the resultant flat plate electroforms should provide some comparative values. The plating conditions for the large flat plate electroforming, irrespective of the bath composition, were as follows:

Volume of Electrolyte: $8 \times 10^{-3} m^3$

Cathode: 10.2 x 15.2 cm mandrel made from 12.7 mm *304* stainless steel. The edges and handle are insulated by a ceramic coating. The plating surface has a polished finish and a flatness within two wavelengths (Fig. *24).*

Anode: The anode has the same dimensions as the cathode, and is fabricated from commerical 1100 aluminum. It is wrapped in a close-woven TFE cloth (which has proved to be superior to the 181 glass cloth for containing the anode slime) (Fig. *24).*
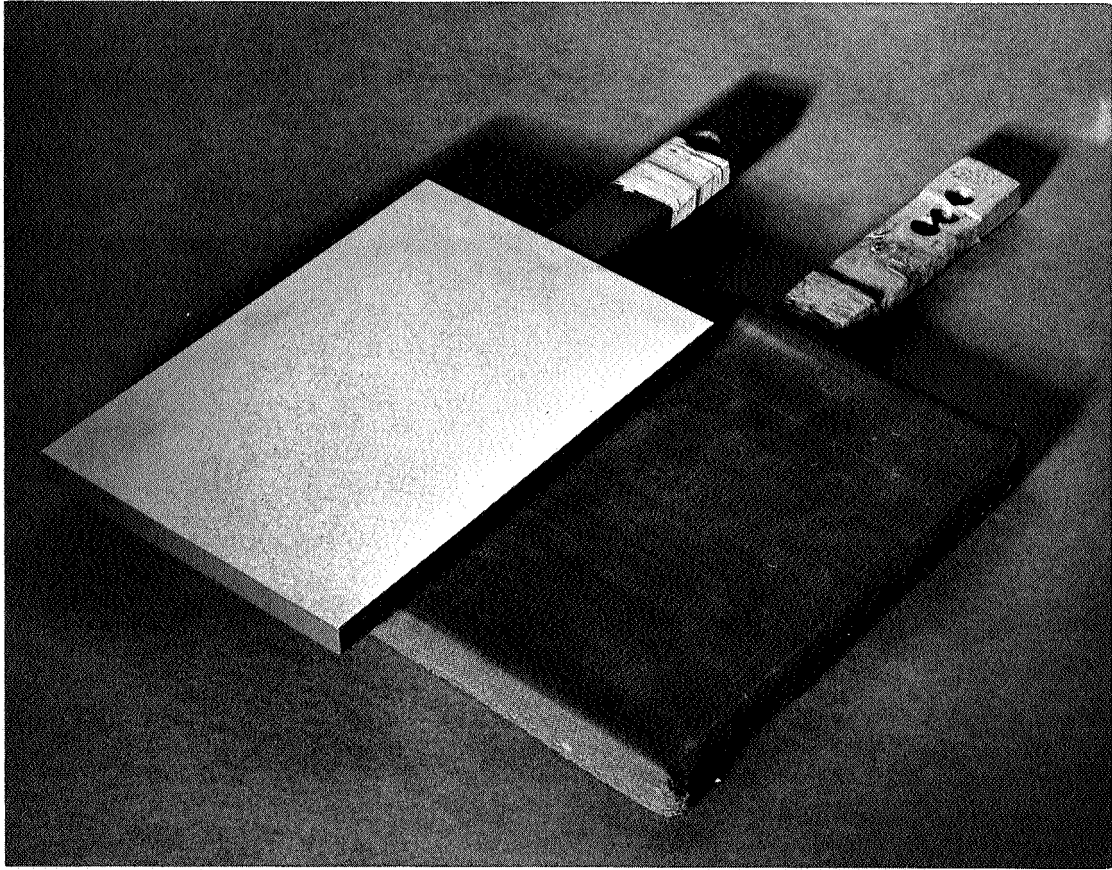
65

Figure *24.*   The Aluminum Anode, Shrouded in TFE Cloth, and the Polished Nickel Cathode for 10.2 x 15.2–cm Flat Plate Electroforming

66

Electrode Distance:	The cathode/anode face-to-face distance was 4.45 cm.
Current Density:	21.6 mA/cm^2.
Equilibrium Temperature:	315°K for the Mg/Al bath
	320°K for the mixed ether bath.

Continuous filtration was employed at a circulation rate of 4×10^{-3} m^3 per minute; the reflux condenser used tap water as the coolant. By replacing the pressure-vacuum filter with continuous circulation combined with use of the reflux condenser, there was practically no loss of bath solvent.

30.5-cm electroformed aluminum mirror. ￭ The 'first attempt in electroforming the mirror was not successful as the deposit was severely stressed and cracked. This was due to wide temperature fluctuations of the bath caused by an improperly adjusted refrigeration unit and by failure of the circulation pump.

The second run was aborted when a short to ground occurred in the motor speed-control circuitry.

The third run was begun with no circulation of solution nor rotation of the mandrel. After an adherent layer of aluminum had been deposited (after 3 hours) rotation and circulation were begun. The resulting mirror contained some blisters which were probably a result of gas trappage at the moment circulation was begun. A fair amount of trees at the center of the mirror is attributed to poor circulation of solution between the mirror and anode pack. The sequence of start-up procedures has been shown to be very critical for good initial adherence and grain structure of the deposit.

Physical properties measurements.

Aluminum: Up to now the criteria used to determine the optimum conditions of plating parameter and the merit of various plating baths were current efficiency, appearance of the resultant deposit, and stability of the plating solution upon electrolysis. Quanti-. tative comparison could only be made by actual physical property measurements. Coupons were made from aluminum flat plates electro-formed from various baths for tensile testing (Fig. 25). The results of the tensile tests are shown in Table VIII.

Emission spectrographic analysis was used to determine the chemical composition of the electrodeposit. Flat plates electro-formed from the bath were analysed to be at least 99.9 percent pure. Table IX is a typical spectrographic analysis. From the result shown in Table VIII and from chemical analysis, the following conclusions may be drawn concerning the aluminum deposit:

- The mixed ether bath yields a deposit with substantially higher physical strength.
- All the components in the magnesium bath have to be added to the aluminum bath to yield a deposit with high physical strength.
- No codeposition of Mg and Al occurs when plating is conducted in the Mg-Al bath.

Additional physical measurements were made on samples from the Al/W Mg component of the magnesium bath and the mixed ether bath to gain some insight on mode of hardening. The results of these tests are shown in Table X. Figure 26 shows an aluminum electro-deposit from the aluminum chloride bath with the added component of the magnesium bath. Figure 27 shows the aluminum electrodeposit from the mixed ether bath. Both photos are magnified 250 times.
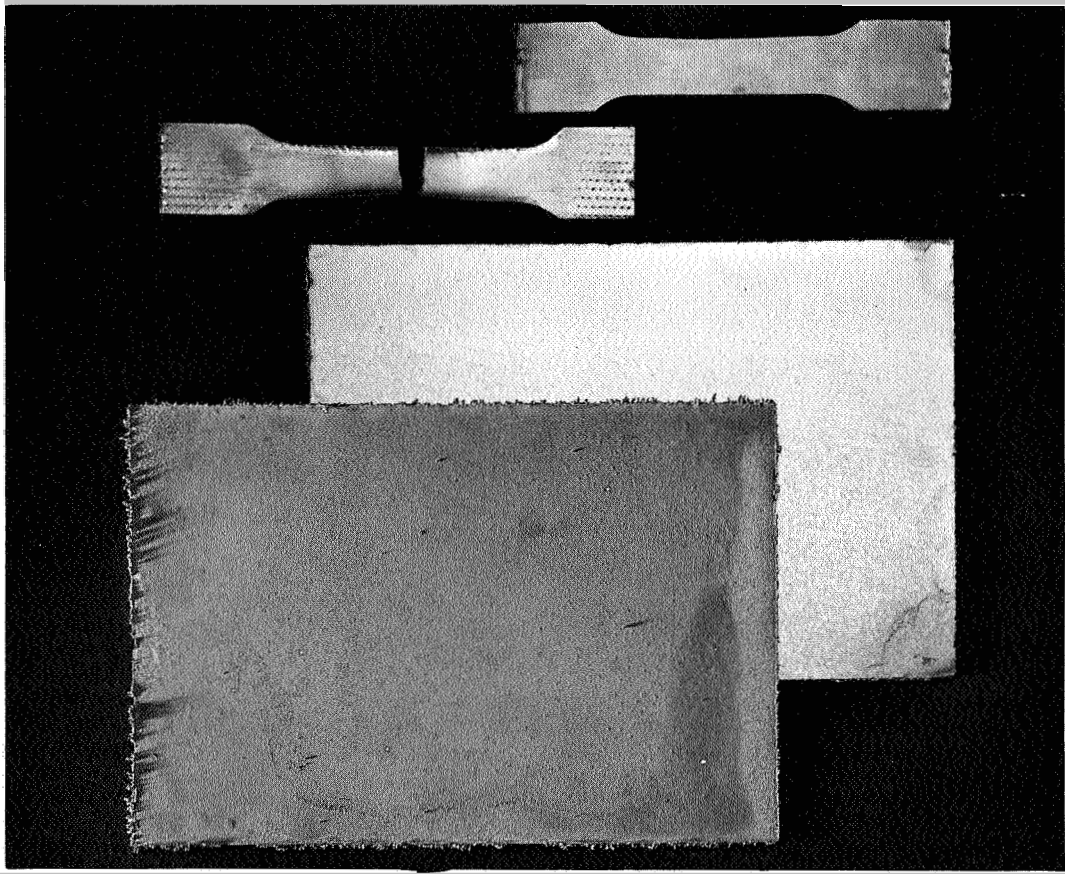
Figure 25. Flat Plate Electroforms and Tensile Test Coupons

TABLE VIII

TENSILE STRENGTH OF ELECTRODEPOSITS
FROM VARIOUS ELECTROPLATING BATHS

	Mg-Al	Al/W Mg-Component	Al/W Mix-Solvent	Mixed-Ether Bath
Yield (MN/m^2) by strain gage	122 (17,600 psi)	75 (10,800 psi)	90 (13,000 psi)	148 (21,400 psi)
Ultimate (MN/m^2)	147 (21,300 psi)	105 (15,200 psi)	118 (17,100 psi)	. 177 (25,700 psi)
% Elongation, 5.08 cm	7	16	18	10

TABLE IX

TYPICAL SPECTROGRAPHIC ANALYSIS

Element	Percent	Element	Percent
Mn	0.011	Pb	< 0.020
Mg	0.0012	Ga	Nil
Si	0.0080	Ni	Nil
cu	0.00018	Ca	0.0011
Fe	< 0.002	Total other elements	Nil
Cr	Nil	Al (by difference)	99.96
Zn	Nil		

TABLE X

COMPARISON OF SOME PHYSICAL PROPERTIES OF DEPOSIT
FROM THE Al-Mg BATH AND THE MIXED ETHER BATH

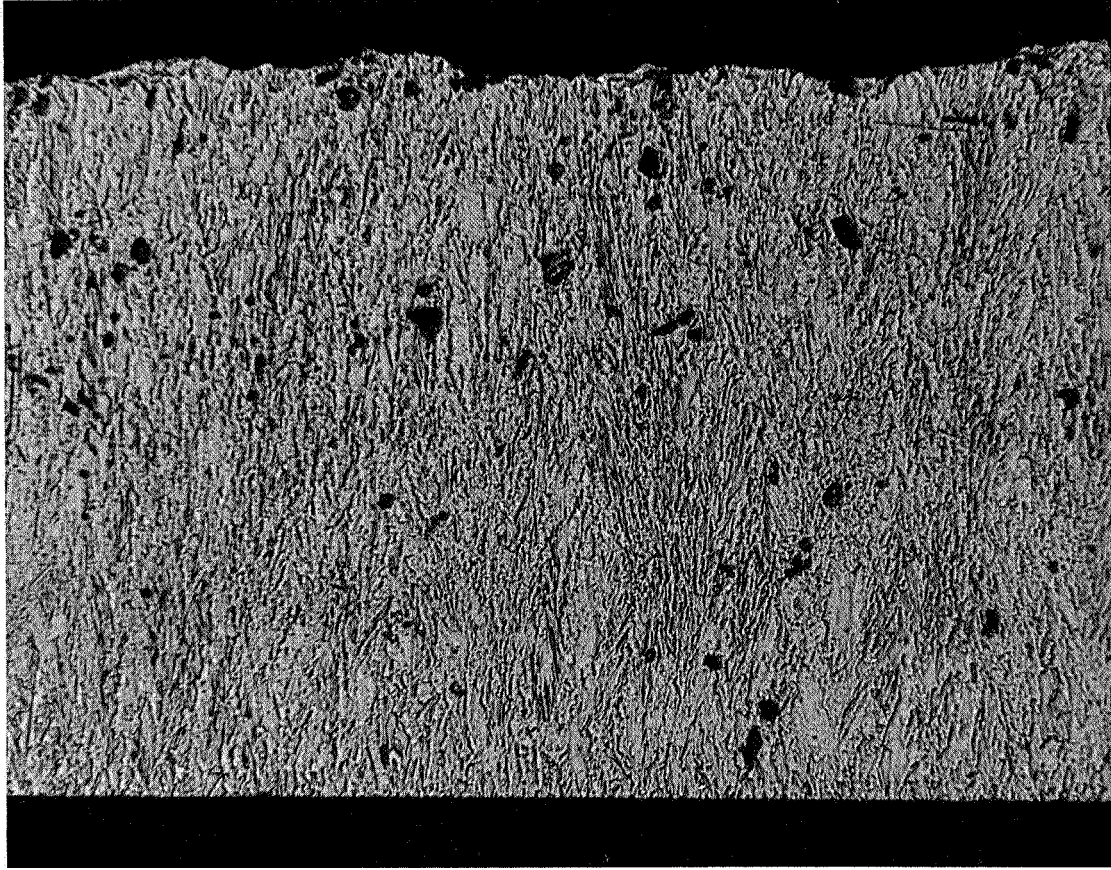|	Al-Mg Bath	Mixed Ether Bath
1. Microhardness tests on polished cross section at 30-gram load	55, **57** with direction of indenter parallel to surface; 48, 50, **55**, with long direction of indenter perpendicular to surface.	71 with long direction of indenter parallel to surface; 68, 71 with indenter perpendicular to surface.
2. Photomicrograph	Fairly compact growth; contains small voids (see Fig. 26).	More compact growth; very few voids (see Fig. 27).
3. X-ray diffraction	Shows only aluminum lines ordered in the 220 direction; no other elements with a strong crystalline structure, with no evidence of amorphous or extremely fine crystal structure.	Shows only aluminum lines with no ordered direction; no other elements with a strong crystalline structure, with no evidence of amorphous or extremely fine crystalline structure.

70

Figure 26. Aluminum Electrodeposit from AlCl$_3$ with Addition of Mg Bath Component (Keller Etch, 250X)
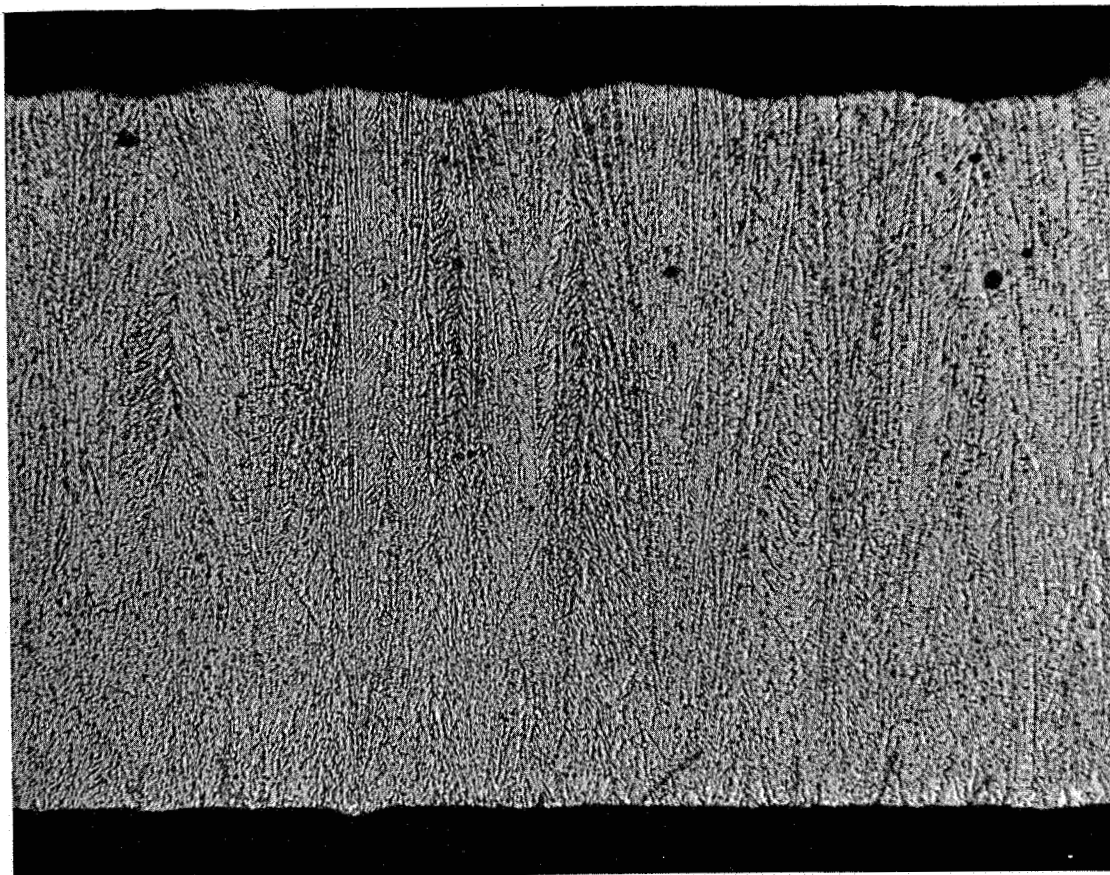
Figure 27. Aluminum Electrodeposit from Mixed Ether Bath
(**Keller** Etch, 250X)

The results of these additional tests may explain the substantial increase of physical strength in light of grain refinement and orientation of growth through change of polarization during metal formation. Metal deposited from the mixed ether bath shows fine grain structure and the absence of ordered crystal orientation. The finer grain structure as revealed by photomicrograph is substantiated by hardness test. Since hardness of electroformed metals is inversely proportional to electroformed grain size, the most desirable deposit for structural purposes is the unoriented microcrystalline structure, which is strongly indicated for the mixed ether deposit through the X-ray diffraction analysis.

Physical measurements were performed on additional flat plates of aluminum electroformed from a mixed ether bath at lower initial bath temperatures ($< 303^{\circ}$K). Average values of yield strength and ultimate strength of 122 MN/m^2 *(17,600* psi) and *140* MN/m^2 (20,100 psi), respectively, were obtained. Average elongation was *4.7%* (5.08 cm). The total effect of temperature (at the start and during plating) upon the crystalline size of the metal electrodeposit has not been completely ascertained. More rigorous temperature control is required. However, the initial plating conditions appear to have a profound effect upon the final electrodeposit.

Magnesium : Physical property measurements were carried out upon 0.12 mm plates (10.2 x 15.2 cm) of electroformed magnesium. The ultimate strengths obtained for three samples were *54* MN/m^2 *(7,830* psi), *53* MN/m$^{\mathbf{2}}$ *(7,650* psi), and *46* MN/m^2 *(6,660* psi). The elongation was 1% (2.54 cm). Results of a typical spectrographic analysis are given in Table XI.

TABLE X I

TYPICAL SPECTROGRAPHIC ANALYSIS OF Mg SAMPLE

Element	Percent
S i	0.02
CU	0.005
Mu	0.01
Fe	0.001
Zn	0.02
Al	0.005
Mg	Remainder

CONCLUSIONS

Electrotechnological Studies

Of the various salt additives investigated for improvement of the conductivity of the magnesium bath, only $MgCl_2$ and tetraethyl-ammonium bromide caused any increase in conductivity--4% at 3 g/$10^{-4}m^3$ (*3* g/100 ml) of bath, and 13% at 5 g/$10^{-4}m^3$ (5 g/100 ml) of bath, respectively. The magnesium deposit from the $MgCl_2$ saturated solution was spongy while that from the solution saturated with tetraethyl-ammonium bromide was fairly coherent.

By addition of alkyl halides to the magnesium bath[*] during plating, dendrite and sponge formation were retarded *so* that relatively thicker deposits of magnesium were obtained. The optimum rate of addition in the case of ethyl bromide was *0.030* mole/hr (15% of the total ampere equivalence) at a plating current density of 10.8 mA/cm^2.

The vapor pressure of the aluminum plating solution was reduced by addition of various higher boiling point ethers[*]. Only two of the resulting higher boiling baths (**3** M $AlCl_3$) yielded a deposit comparable to that of the normal aluminum bath. These were diethyl ether-anisole (2:1, bp=3o7°K) and diethyl ether - bis (2-chloroethyl) ether (2:1, bp=375°K).

Exposure of the normal aluminum plating solution to the atmosphere for short duration (less than one minute) had no ill

---

*The sources and purities of bath constituents are given in Appendix B.

effect upon the electrodeposit. However, solutions exposed for a
long duration **(1800** seconds) either yielded poor deposits or
completely decomposed.

A study was made to determine the operable current density range
for the magnesium and the magnesium-aluminum baths without deleteri-
ous effects upon the electrodeposit. The optimum current density in
terms of overall quality of deposit was 10 to 15 mA/cm^2 for the magne-
sium bath and 20 to *40* mA/cm^2 for the magnesium-aluminum bath.

The use of periodic current reversal was investigated in an
attempt to minimize roughness and nodule formation during formation
of relatively thick deposits of aluminum (greater than **0.38** mm).
The optimum forward-to-reverse ratio appeared to be near 20:1 (i.e.,
180 seconds plating and 9 seconds deplating) at a current density
of 11 mA/cm^2.

Electrode studies with the aluminum bath showed that aluminum
is anodically dissolved at almost 100% current efficiency. However,
some phenomena exist during the plating process that cause
variation in the bath characteristic over long periods of time.
In the case of the magnesium bath, magnesium was not anodically
dissolved during plating and addition of ethyl bromide was required
to replenish the magnesium in solution.

Alloying Studies

Solubility and conductivity tests in diethyl ether and the
aluminum plating solution were performed on anhydrous salts of
metals most likely to codeposit with aluminum: Ti, Mg, Cu, Be,
Mn, and Sn. **A** total **of 35** salts were tested. The anodic and

76

cathodic decomposition voltages for the magnesium plating solution
were found to be -1.45V and +0.65V, respectively (in reference to a
platinum wire electrode).

Polarization curve measurements were peformed on seven titanium
salts in diethyl ether to determine decomposition potentials.. The
curves obtained were very similar to those of the normal aluminum
plating solution. Any additional plateaus were probably obscured
when the data was plotted.

The use of cyclic sweep voltammetry (triangular voltage-time
sweep) for studying the electrochemical characteristics of the
plating solutions was attempted. However, equipment deficiencies
and limitations prevented accumulation of any meaningful data.

Process Development

A laboratory plating assembly was constructed for the electro-
forming of magnesium mirrors. The entire system is closed, air-
tight, and made of glass. The essential features are bath agitation,
continuous bath filtration, continuous bath concentration replenish-
ment, and continuous addition of alkyl halide.

A safety engineered bunker was constructed for plating of the
30.5-cm aluminum mirror. The cell for electroforming the mirror
includes provisions for rotating the nickel master while plating.
Continuous filtration and circulation also are incorporated into
the system. Solvent losses are minimized by a stainless steel
reflux-condenser lid.

Electroforming Studies

Flat plates of aluminum (10.2 x 15.2 cm) were electroformed from both the magnesium–aluminum bath and the mixed ether (high boiling) bath. Plating in the magnesium–aluminum bath (a mixture of the aluminum bath and magnesium bath) resulted in a deposit that was considerably stronger than that obtained from the aluminum bath. Spectrographic analysis of the resultant plates indicated that codeposition of magnesium with aluminum did not occur.

Flat plates electroformed from the mixed ether bath (yield strength, 148 MN/m^2 (21,300 psi) were even stronger and harder than those from the **Mg-Al** bath (yield strength, 121 MN/m^2 (17,600 psi)). The purity of the aluminum deposit was at least 99.9 percent.

A 30.5–cm parabolic aluminum mirror was also electroformed from the mixed–ether bath.

APPENDIX A

PROGRAM STATEMENT OF WORK

A   ELECTROTECHNOLOGY STUDIES

1.   Bath Composition

   a.   Improved conductivity shall be studied by the addition of
         such suitable ionizing salt additives as tetraethyl
         ammonium halides, lithium borohydride, lithium aluminum
         hydride, magnesium halides, etc.

   b.   Reduction of bath vapor pressure shall be studied by the
         addition of higher boiling point organics of the ether
         family.

   c.   Increased magnesium yield shall be studied by the addition
         of reactive chemical species.

   d.   The effects of contaminants such as water, oxygen and
         solvent impurities shall be investigated.

   e.   The efficacy of nonparticipating additives for improving
         plating characteristics shall be investigated with
         compatible organic and inorganic liquids.

2.   Electrode Studies

   a.   An evaluation of anode chemical reversibility shall be
         studied. One approach shall be the proper addition of
         an organo halide chemical reactant.

   b.   The effects of current density on the microcrystalline
         structure and dendritic formation shall be investigated.

   c.   The effect of reverse cycle depolarization on dendritic
         formation shall be investigated.

   d.   Tests shall be conducted to achieve deposit thicknesses
         greater than 0.76 mm in both the magnesium and aluminum
         baths.

3. Physical Properties Measurements

    a.   Tests shall be made on flat samples to determine tensile yield strength, ultimate strength and modulus of elasticity as well as Vickers hardness.

    b.   Chemical analysis shall be made of each sample on which physical properties are measured. Emission spectrography and wet chemical techniques shall be employed.

    c.   Metallographic photographs shall be taken on selected samples having desirable properties. Where required, X-ray evaluation of crystal structure shall be made.

4. Alloying Studies

Varying concentrations of the magnesium bath in the aluminum bath shall be evaluated as to their efficacy in enhancing the properties of the resulting deposits. Where suitable, other organo metallics shall be employed to enhance deposit characteristics.

B.   <u>PROCESS DEVELOPMENT</u>

This phase shall be devoted primarily to studying the conversion of the electroforming process from a laboratory operation to a pilot plant operation. Such techniques as continuous renewal of the plating bath, scale-up problems (controls safety, size) and structural material compatibility shall be studied.

C.   <u>ELECTROFORMING STUDIES</u>

In this phase of the program, the practicality of the bath or baths developed under paragraph A., <u>Electrotechnology Studies</u>, shall be demonstrated. The demonstration shall consist of the fabrication

of at least one 30.5-cm diameter paraboloid for each of the baths chosen. In the process of fabricating the paraboloid, electrode configuration problems shall be determined by an investigation of the throwing-power of the anode.

APPENDIX B

PURITY OF MATERIALS USED IN ALUMINUM PLATING SOLUTION

Chemical	Grade	Source
Diethyl ether, anhydrous	Reagent	Allied Chemical Corp., Morristown, N. J.

Maximum limits of impurities:

Water	0.010%
Peroxides (as H_2O_2)	0.00005%
Acid (as CH_3COOH)	0.0010%
Aldehyde (as HCHO)	0.0005%
Heavy metals (as Pb)	0.0001%
Residue after evaporation	0.0010%

Chemical	Grade	Source
Anisole	Baker (99% Min.)	J. T. Baker, Phillipsburg, N. J.

Maximum limits of impurities:

Phenol	0.2%
Water	0.5%

Chemical	Grade	Source
Aluminum chloride, anhydrous	Reagent (99.0% Min.)	Allied Chem. Corp., Morristown, N. J.

Maximum limits of impurities:

Sulfate	0.003%

Heavy metals (as Pb)	*0.002%*	
Iron	0.010%	
Substances not pptd by NH_4OH	*0.20%*	
Lithium aluminum hydride, powder	*95%* Min.	Metal Hydrides, Inc., Beverly, Mass.

Typical impurities:

LiCl	*2.0 - 2.5%*
$LiAlO_2$	1.0 - *2.0%*
$(CH_3CH_2)_2O$	0.1 - *0.2%*
AlH_3	0.1 - *0.2%*

PURITY OF MATERIALS USED IN MAGNESIUM PLATING SOLUTION

Tetrahydrofuran	Reagent	J. T. Baker, Phillipsburg, N. J.

Impurities:

Water	*0.025%*
Peroxides (as H_2O_2)	*0.005%*
Preservative	*0.025%*

Ethyl magnesium bromide, 3.0M, in ethyl ether	Reagent	Arapahoe Chemical, Boulder, Colo.
Ethyl bromide	Reagent	J. T. Baker, Phillipsburg, N.J.

Impurities:

Chloroform	0.010%
Other bromides	0.0005%
Residue after evaporation	0.001%

ABSTRACT

Studies to optimize organic solvent plating baths for the deposition of aluminum and magnesium were conducted. The program was divided into electrotechnology studies, process development, and electroforming studies. High purity aluminum was electroformed from a mixed ether bath of aluminum chloride and lithium aluminum hydride which showed potentially useful structural characteristics. High purity magnesium was also successfully electroformed. The effects of current density bath impurities and various solvent and salt additions were studied. The aluminum electroforming process was scaled up and an aluminum paraboloid mirror, 30.5 centimeters, was electroformed to demonstrate the practicability of the bath.

a4